 IEEE Transactions on Signal Processing, vol. 61, no. 16, Aug. 2013, pp. 4051–4066

IDMA for the Multiuser MIMO-OFDM Uplink: A Factor Graph Framework for Joint Data Detection and Channel Estimation

Clemens Novak, Gerald Matz, *Senior Member, IEEE,* and Franz Hlawatsch, *Fellow, IEEE*

***Abstract*—Interleave-division multiple access (IDMA) has recently been proposed as a promising alternative to code-division multiple access (CDMA). In this paper, we consider the use of IDMA within a multiple-input multiple-output orthogonal frequency-division multiplexing (MIMO-OFDM) multiuser system employing higher-order modulation and transmitting over frequency-selective MIMO channels. Based on a factor graph/message passing framework and the sum-product algorithm, we devise an iterative receiver that jointly performs pilot-aided channel estimation, multiuser detection, and channel decoding. The use of Gaussian message approximations results in a receiver complexity that scales only linearly with the number of users. A further complexity reduction is obtained by a novel selective message updating scheme. We also present a simulation-based comparison of the maximum rate achievable with our MIMO-OFDM-IDMA receiver with the information-theoretic capacity of the multiple-access channel. Finally, we provide simulation results illustrating the bit error rate (BER) performance of our receiver. It is observed that the proposed turbo-like integration of channel estimation in the iterative multiuser detection and channel decoding scheme yields a dramatic BER reduction, and that the proposed selective message updating scheme results in a significant reduction of complexity.**

***Index Terms*—Belief propagation, channel estimation, factor graph, IDMA, interleave-division multiple access, iterative receiver, message passing, MIMO-IDMA, MIMO-OFDM, multiple access, multiuser detection, spatial multiplexing, sum-product algorithm.**

I. Introduction

A. Background and State of the Art

THIS paper considers a multiuser multiple-input multiple-output (MIMO) uplink scenario where several users transmit data to a common base station over frequency-selective MIMO channels. Base station and users are equipped with multiple antennas, and user separation is achieved by means of a recently introduced technique known as interleave-division multiple access (IDMA) [1]. With IDMA, users are separated via user-specific interleavers combined with low-rate channel coding. This is in contrast to code-division multiple access (CDMA), where users are separated by means of user-specific spreading sequences [2]. While CDMA and IDMA both offer the potential to achieve diversity gains and to mitigate inter-cell interference, IDMA has some important advantages over CDMA: it enables the use of multiuser detectors that are significantly less complex than those required for CDMA [1], [3]–[7], and it can outperform coded CDMA when iterative (turbo) receivers are used [1], [4], [7]. Furthermore, IDMA can be easily integrated into MIMO systems [8], and frequency-selective channels can be accommodated by combining IDMA with orthogonal frequency-division multiplexing (OFDM) [9]–[11]. Interleaver design for IDMA was discussed in [12] and [13]. An ad hoc receiver design incorporating channel estimation for a BPSK-modulated single-antenna IDMA system was presented in [14]. An extension of IDMA termed multi-layer IDMA was proposed in [15]. A more detailed introductory discussion of IDMA and further references can be found, e.g., in [3] and [15].

In coded multiuser systems, large performance gains can be achieved by using an iterative turbo-style interaction between multiuser detector and channel decoder [16], [17]. Previous work on iterative IDMA receiver design [1], [7], [14], [15] used minimum mean square error or soft rake equalizers and was limited either to single-antenna systems or to BPSK modulation or to the case of perfect channel state information (CSI) at the receiver. In this paper, by contrast, we consider MIMO-IDMA systems with higher-order modulation to achieve increased spectral efficiency, and we use OFDM as the modulation format to accommodate frequency-selective (time-dispersive) channels. For this transmission scenario, we develop an iterative receiver using a factor graph/message passing framework [18]–[20]. Via Gaussian approximations [18], [19], we modify the sum-product algorithm to obtain a computationally efficient message-passing receiver that performs joint multiuser detection, channel decoding, and pilot-aided channel estimation, and whose complexity scales only linearly with the number of users.

Our factor graph based receiver design follows the approach proposed in [17], [20], [21], which has recently been pursued for various transmission scenarios (but not for MIMO-OFDM-IDMA). More specifically, [22]–[24] have dealt with joint data detection and channel estimation in single-user single-antenna systems with flat fading, whereas the case of frequency-selective channels has been addressed in [25]–

C. Novak was with the Institute of Telecommunications, Vienna University of Technology, A-1040 Vienna, Austria. He is now with Kapsch TrafficCom, A-1120 Vienna, Austria (email: clemens.novak@kapsch.net).

G. Matz and F. Hlawatsch are with the Institute of Telecommunications, Vienna University of Technology, A-1040 Vienna, Austria (email: {gmatz, fhlawats}@nt.tuwien.ac.at).

This work was supported by the STREP project MASCOT (IST-026905) within the Sixth Framework of the EC and by the FWF projects "Statistical Inference" (S10603) and "Information Networks" (S10606) within the National Research Network SISE.

[27] and—augmented with sparsity-exploiting techniques—in [28]. Message-passing receivers for joint detection and channel estimation in single-user MIMO-OFDM systems have been studied in [29] and [30]. Based on a similar factor graph framework, low-complexity soft-input/soft-output detection for linear channels (MIMO, doubly dispersive, etc.) has been investigated in [31].

We furthermore propose a novel threshold-based selective message update scheme to further reduce the complexity of the iterative receiver. Related ideas to reduce the number of message updates have been proposed for belief propagation decoders for LDPC codes in [32]–[38]. Apart from being formulated for LDPC decoders, these papers differ from our method in that they do not use the posterior log-likelihood ratio in the update criterion, do not consider designs with a prescribed (fixed) complexity, and do not observe a simultaneous complexity reduction and performance improvement.

B. Contributions and Paper Organization

The main contribution of this paper is the combination of MIMO-OFDM-IDMA with a factor graph based design of iterative message passing receivers that perform joint detection/decoding and channel estimation. Our specific contributions can be summarized as follows.

- *Iterative MIMO-OFDM-IDMA receiver.* We propose a receiver for MIMO-OFDM-IDMA with higher-order modulation. This receiver can be viewed as a reduced-complexity approximation of the maximum a posteriori (MAP) detector, which is optimal in the sense of minimum error probability but computationally infeasible. We first develop a factor graph representation of the MIMO-OFDM-IDMA system; then, we use this factor graph and the sum-product algorithm to compute the marginal probabilities required by the MAP detector. Since the complexity of the sum-product algorithm grows exponentially with the number of users, we propose approximations for some of the messages to obtain a complexity that scales only linearly with the number of users.
- *Integrated channel estimation.* Pilot-aided channel estimation is usually employed at the receiver to obtain an estimate of the CSI required by the multiuser detector. Rather than estimating the coefficients of the frequency-selective MIMO channels only once, our factor graph based receiver incorporates pilot-aided channel estimation into the factor graph and the sum-product algorithm, thereby obtaining a successive refinement of the channel estimates in the course of the receiver iterations. Thus, our receiver performs iterative joint multiuser data detection/decoding and channel estimation for pilot-aided MIMO-OFDM-IDMA.
- *Selective message updating.* We propose a selective message update scheme in which only a subset of the messages is updated in each iteration of the sum-product algorithm. The messages are represented by log-likelihood ratios (LLRs), and the LLRs to be updated are determined adaptively via an LLR threshold. This yields a significant reduction of computational complexity and makes it possible to trade error performance against computational efficiency in a flexible manner. Our selective message update scheme typically leads to a complexity reduction by a factor of 2 to 3 and, surprisingly, in certain cases to a simultaneous bit error rate (BER) improvement by one order of magnitude.
- *Performance assessment.* We consider the information rate achievable with IDMA as a performance metric and compare it with the information-theoretic capacity of the multiple-access channel. To obtain estimates of the achievable rates of IDMA, we determine the signal-to-noise ratio (SNR) thresholds achieved with our low-complexity iterative IDMA receiver combined with an LDPC channel code of a given rate. We furthermore provide simulation results to illustrate the performance gains of our receiver relative to conventional IDMA receivers. It is observed, in particular, that inclusion of channel estimation in the iterative detection/decoding scheme yields a dramatic improvement of reliability, and selective message updating yields a significant reduction of complexity.

We note that we have previously considered MIMO-IDMA with turbo-demodulation [8], joint detection and channel estimation for IDMA in flat-fading channels [39], IDMA with higher-order modulation and selective LLR updates [40], and OFDM-IDMA [11]. However, none of these previous conference papers presented the full combination of joint detection-estimation for MIMO-OFDM-IDMA with higher-order modulation and selective message updates. Furthermore, these publications provided neither an assessment of the achievable IDMA sum rate nor a selective message update scheme with fixed complexity.

This paper is organized as follows. The system model and the IDMA transmitter and demodulator are presented in Section II. In Section III, we construct the factor graph of our system and derive the messages to be propagated along the edges of the factor graph. Section IV develops message approximations and a selective message update scheme. The achievable sum rates of IDMA are studied in Section V. Finally, Section VI demonstrates the performance of the proposed receiver by means of numerical simulations.

II. MIMO-OFDM-IDMA System Model

We consider a MIMO-OFDM-IDMA system for an uplink multiple-access scenario with U users. Each user employs M_{T} transmit antennas for spatial multiplexing [41], and the base station is equipped with M_{R} receive antennas. Frequency-selective Rayleigh fading channels are assumed, and the equivalent discrete-time complex baseband domain (with symbol-rate sampling) is considered throughout.

A. Transmitter

The MIMO-OFDM-IDMA transmitter for the uth user is shown in Fig. 1. This transmitter extends the BPSK-based

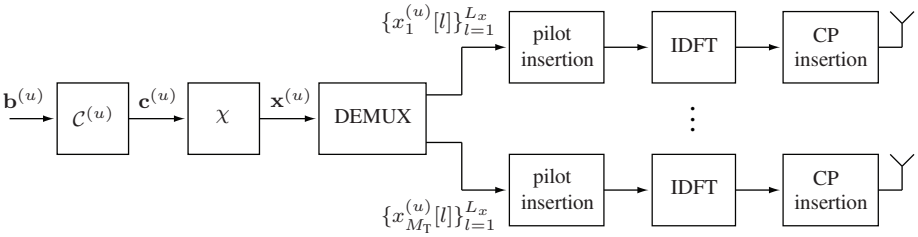

Fig. 1. MIMO-OFDM-IDMA transmitter for the uth user.

MIMO-IDMA transmitter of [8] to OFDM modulation and higher-order symbol alphabets.

1) Coding, interleaving, mapping: A length-J sequence of information bits of the uth user, denoted as $\mathbf{b}^{(u)} \triangleq \big(b_1^{(u)} \cdots b_J^{(u)}\big)^T$, with $u \in \{1,\ldots,U\}$, is encoded into a length-L sequence of code bits. We assume that all information bit sequences $\mathbf{b}^{(u)} \in \{0,1\}^J$ are equally likely. The code is a concatenation of a terminated, systematic convolutional code of rate $R_1 = J/\tilde{L}$ and a repetition code of (typically very low) rate $R_2 = \tilde{L}/L$. We assume $L > \tilde{L} > J$. The overall code rate equals $R = R_1 R_2 = J/L < 1$. The code bit sequence is then passed through a user-specific interleaver $\pi^{(u)}$, which yields the interleaved bit sequence $\mathbf{c}^{(u)} \triangleq \big(c_1^{(u)} \cdots c_L^{(u)}\big)^T$. We can express $\mathbf{c}^{(u)}$ as

$$\mathbf{c}^{(u)} = \mathcal{C}^{(u)}(\mathbf{b}^{(u)}), \tag{1}$$

where the one-to-one function $\mathcal{C}^{(u)}(\cdot)$ characterizes the combined effect of channel coding and interleaving. Different users employ identical codes but different interleavers. The combination of low-rate repetition code and user-specific interleaver replaces the spreading employed in CDMA systems.

Next, the coded and interleaved bit sequence $\mathbf{c}^{(u)}$ is mapped to a sequence of $L_x = L/(M_\mathrm{T}B)$ complex symbol vectors $\mathbf{x}^{(u)}[l] \triangleq \big(x_1^{(u)}[l] \cdots x_{M_\mathrm{T}}^{(u)}[l]\big)^T$, $l = 1,\ldots,L_x$; here, B is the number of bits per scalar symbol, which is related to the size of the symbol alphabet $\mathcal{S}$ according to $|\mathcal{S}| = 2^B$. The transmit symbol $x_i^{(u)}[l] \in \mathcal{S}$ at the ith antenna ($i \in \{1,\ldots,M_\mathrm{T}\}$) of the uth user at symbol time l is obtained by mapping B successive interleaved code bits $c_{\lambda(l,i)+1}^{(u)},\ldots,c_{\lambda(l,i)+B}^{(u)}$, with $\lambda(l,i) \triangleq \big[(l-1)M_\mathrm{T} + i - 1\big]B$, to a symbol from $\mathcal{S}$. This mapping operation will be denoted as

$$x_i^{(u)}[l] \;=\; \chi\big(\mathbf{c}_i^{(u)}[l]\big), \tag{2}$$

with the one-to-one symbol mapping χ and the bit vector (*symbol label*) $\mathbf{c}_i^{(u)}[l] \triangleq \big(c_{\lambda(l,i)+1}^{(u)} \cdots c_{\lambda(l,i)+B}^{(u)}\big)^T \in \{0,1\}^B$. With a slight abuse of notation, the transmit symbol vector (across the antennas) of the uth user at symbol time l will be similarly written as

$$\mathbf{x}^{(u)}[l] \;=\; \chi\big(\mathbf{c}^{(u)}[l]\big), \tag{3}$$

where $\mathbf{c}^{(u)}[l] \triangleq \big(\mathbf{c}_1^{(u)T}[l] \cdots \mathbf{c}_{M_\mathrm{T}}^{(u)T}[l]\big)^T$.

2) OFDM modulation and pilot insertion: The data symbols $x_i^{(u)}[l]$, $l = 1,\ldots,L_x$, are transmitted at the ith antenna of the uth user by means of OFDM modulation, i.e., the lth symbol $x_i^{(u)}[l]$ modulates a corresponding subcarrier k. In addition, to enable channel estimation, each user employs $M_\mathrm{T}K_p$ pilot subcarriers. Assuming that the pilot subcarriers of different users are disjoint whereas L_x information-bearing subcarriers are shared among all users, the total number of subcarriers equals

$$K \triangleq L_x + UM_\mathrm{T}K_p\,. \tag{4}$$

The symbol (data or pilot) of user u that is transmitted at antenna i and subcarrier $k \in \{0,\ldots,K-1\}$ is denoted as $s_i^{(u)}[k]$. Furthermore, the (data or pilot) symbol vector associated with subcarrier k and comprising all antennas is denoted as $\mathbf{s}^{(u)}[k] \triangleq \big(s_1^{(u)}[k] \cdots s_{M_\mathrm{T}}^{(u)}[k]\big)^T$. The time-domain signal of the uth user transmitted at the ith antenna is obtained by applying an inverse discrete Fourier transform (IDFT) of length K to the symbol sequence $\{s_i^{(u)}[k]\}_{k=0}^{K-1}$ and inserting a cyclic prefix of length N_cp.

3) Pilot and data arrangement: We use the arrangement of data and pilot subcarriers shown in Fig. 2. A given user employs K_p pilot subcarriers for a given antenna; thus, the total number of pilot subcarriers (for all users and transmit antennas) is $UM_\mathrm{T}K_p$, which we assume to be much smaller than K (cf. (4)). The number K_p of pilots per user and per antenna is usually chosen to be larger than the maximum length of the impulse responses of all user channels. The $UM_\mathrm{T}K_p$ pilot subcarriers are arranged in K_p blocks, each containing UM_T pilot subcarriers (one for each user and transmit antenna). More specifically, the K_p pilot subcarriers for a given user and transmit antenna are located in K_p different blocks that are spaced $\Delta = \lfloor \frac{K}{K_p - 1} \rfloor$ subcarriers apart (see Fig. 2). Each pilot subcarrier is used only by one user for one transmit antenna whereas each data subcarrier is used jointly by all users and all transmit antennas.[1] The set of pilot subcarriers employed by the uth user for the ith antenna is given by $\mathcal{P}_i^{(u)} \triangleq \{(u-1)M_\mathrm{T} + i + \kappa\Delta - 1 \,|\, \kappa = 0,\ldots,K_p - 1\}$;

[1]This choice has been made for simplicity of exposition. The receiver developed in what follows can be easily generalized to the case where different users employ the same pilot subcarriers.

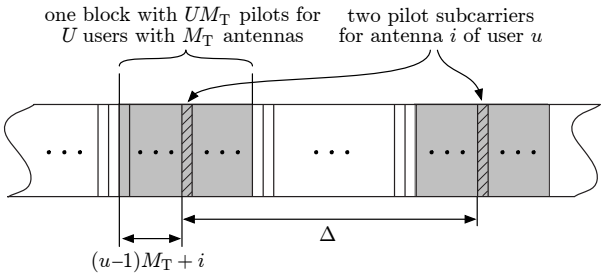

Fig. 2. Arrangement of data subcarriers (white) and pilot subcarriers (grey). Two pilot blocks (grey) of length UM_T spaced Δ subcarriers apart are shown.

note that $|\mathcal{P}_i^{(u)}| = K_p$. The pilot symbols are chosen equal for all users and antennas, therefore $\mathbf{s}^{(u)}[k] = p\,\mathbf{e}_i$ for $k \in \mathcal{P}_i^{(u)}$, where p is the common pilot symbol and $\mathbf{e}_i$ denotes the ith unit vector of length M_T. Note that for $k \in \mathcal{P}_i^{(u)}$, the symbols at all other antennas are zero, i.e., $s_{i'}^{(u)}[k] = 0$ for $i' \neq i$. Finally, the union of all the (disjoint) sets $\mathcal{P}_i^{(u)}$ will be denoted as $\mathcal{P}$; note that $|\mathcal{P}| = UM_\mathrm{T}K_p$.

The data symbols $x_i^{(u)}[l]$ are mapped to the data subcarrier symbols according to

$$s_i^{(u)}[k] = x_i^{(u)}[\ell_k]\,, \quad \text{for } k \notin \mathcal{P},\ i \in \{1,\ldots,M_\mathrm{T}\},\ u \in \{1,\ldots,U\},$$

where ℓ_k denotes the index of the symbol that is mapped to subcarrier k.

4) Spectral efficiency: We define the spectral efficiency for one user as the ratio of the number of information bits J to the number of subcarriers K, i.e., $\epsilon \triangleq J/K$. Using the definitions and relations provided previously, we obtain

$$\epsilon \;=\; M_\mathrm{T}BR\left(1 - \frac{UM_\mathrm{T}K_p}{K}\right).$$

Here, the expression in parentheses quantifies the loss in spectral efficiency due to the pilot symbols. For fixed K, the spectral efficiency decreases when the number U of users increases. Decreasing the number K_p of pilots improves the spectral efficiency but results in a poorer initial channel estimate and hence may necessitate a larger number of receiver iterations to achieve a performance target.

B. Channel and Demodulation

We assume frequency-selective fading and denote by $L_\mathrm{ch}{-}1$ the maximum discrete-time delay of all user channels (we assume hereafter that the cyclic prefix length satisfies $N_\mathrm{cp} \geq L_\mathrm{ch}$). The impulse response of the MIMO channel between user u and the base station is given by the $M_\mathrm{R} \times M_\mathrm{T}$ matrix sequence $\widetilde{\mathbf{H}}^{(u)}[\nu]$, $\nu = 0,\ldots,L_\mathrm{ch}-1$. Sometimes it will be convenient to use the length-L_ch impulse response vector between the ith transmit antenna of user u and the jth base station antenna given by $\tilde{\mathbf{h}}_{j,i}^{(u)} \triangleq \big(\tilde{h}_{j,i}^{(u)}[0] \cdots \tilde{h}_{j,i}^{(u)}[L_\mathrm{ch}-1]\big)^T$; here $\tilde{h}_{j,i}^{(u)}[\nu]$ denotes the (j,i)th element of $\tilde{\mathbf{H}}^{(u)}[\nu]$. The channel tap vectors $\tilde{\mathbf{h}}_{j,i}^{(u)}$ are assumed mutually independent and zero-mean complex Gaussian, i.e., $\tilde{\mathbf{h}}_{j,i}^{(u)} \sim \mathcal{CN}(\mathbf{0}, \mathbf{C}_{\tilde{h}})$, where $\mathbf{C}_{\tilde{h}}$ is a diagonal $L_\mathrm{ch} \times L_\mathrm{ch}$ matrix whose diagonal elements correspond to the power delay profile (for simplicity assumed identical for all users and antenna pairs). The associated frequency-domain channel coefficient vector is given by

$$\mathbf{h}_{j,i}^{(u)} \triangleq \big(h_{j,i}^{(u)}[0] \cdots h_{j,i}^{(u)}[K-1]\big)^T = \mathbf{F}\tilde{\mathbf{h}}_{j,i}^{(u)}\,, \qquad (5)$$

where the $K \times L_\mathrm{ch}$ matrix $\mathbf{F}$ consists of the first L_ch columns of the $K \times K$ unitary DFT matrix, i.e., its elements are given by $(\mathbf{F})_{k\nu} = \frac{1}{\sqrt{K}} \exp\big(-\frac{j2\pi k\nu}{K}\big)$ for $k \in \{0,\ldots,K-1\}$ and $\nu \in \{0,\ldots,L_\mathrm{ch}-1\}$.

The receiver first removes the cyclic prefix and then performs a length-K DFT of the received signal. This results in the frequency-domain receive vector sequence $\mathbf{r}[k]$, $k = 0,\ldots,K-1$, which consists of L_x vectors at the data subcarriers $k \notin \mathcal{P}$ and $UM_\mathrm{T}K_p$ vectors at the pilot subcarriers $k \in \mathcal{P}_i^{(u)}$, i.e.,

$$\mathbf{r}[k] \;=\; \begin{cases} \sum_{u=1}^{U} \mathbf{H}^{(u)}[k]\,\mathbf{x}^{(u)}[\ell_k] + \mathbf{w}[k]\,, & k \notin \mathcal{P}, \\ \mathbf{H}^{(u)}[k]\,\mathbf{s}^{(u)}[k] + \mathbf{w}[k]\,, & \\ \quad k \in \mathcal{P}_i^{(u)}, u \in \{1,\ldots,U\},\ i \in \{1,\ldots,M_\mathrm{T}\}\,. \end{cases} \qquad (6)$$

Here, $\mathbf{H}^{(u)}[k]$, $k = 0,\ldots,K-1$, is the length-K unitary DFT of the time-domain channel impulse response $\widetilde{\mathbf{H}}^{(u)}[\nu]$, $\nu = 0,\ldots,L_\mathrm{ch}-1$ (zero-padded to length K) and $\mathbf{w}[k]$ is a white noise sequence whose elements are independent and identically distributed (i.i.d.) Gaussian with zero mean and variance σ_w^2. Since the pilot vector for $k \in \mathcal{P}_i^{(u)}$ was chosen as $\mathbf{s}^{(u)}[k] = p\,\mathbf{e}_i$, the receive vectors at the pilot subcarriers are given by

$$\mathbf{r}[k] \;=\; \mathbf{H}^{(u)}[k]\,p\,\mathbf{e}_i + \mathbf{w}[k] \;=\; p\mathbf{h}_i^{(u)}[k] + \mathbf{w}[k]\,, \quad k \in \mathcal{P}_i^{(u)}, \qquad (7)$$

where $\mathbf{h}_i^{(u)}[k] \triangleq \mathbf{H}^{(u)}[k]\,\mathbf{e}_i$ is the ith column of the channel matrix $\mathbf{H}^{(u)}[k]$.

The K vectors $\mathbf{r}[k]$ of length M_R are stacked into the overall receive vector $\mathbf{r} \triangleq \big(\mathbf{r}^T[0] \cdots \mathbf{r}^T[K{-}1]\big)^T$ of length KM_R. This vector is the basis for the receiver processing steps discussed in Sections III and IV.

III. Factor Graph Framework for MIMO-OFDM-IDMA

Factor graphs are an intuitively appealing tool for representing the factorization of a function (e.g., probability density) of many variables [18]. Marginals of the function can be efficiently computed by means of the sum-product algorithm [18], [19], which is a message-passing algorithm on the factor graph. Here, we will apply the factor graph framework to the design of a full-blown receiver for MIMO-OFDM-IDMA. Based on an analysis of the statistical structure of the MIMO-OFDM-IDMA system, we will construct the corresponding factor graph and derive the messages to be propagated along its edges according to the sum-product algorithm. This will lead quite naturally to an iterative message-passing algorithm for joint data detection, channel decoding, and pilot-aided channel estimation.

A. Derivation of the Factor Graph

The MIMO-OFDM-IDMA receiver processes the overall receive vector $\mathbf{r}$ and provides detected information bits $\hat{b}_m^{(u)}$, $m = 1,\ldots,J$, for all users $u = 1,\ldots,U$. The receiver we propose is an approximation of the optimal (in the sense of minimum bit error probability) MAP bit detector [21], [42]

$$\hat{b}_m^{(u)} = \underset{b_m^{(u)} \in \{0,1\}}{\operatorname{argmax}}\ p(b_m^{(u)}|\mathbf{r}) = \mathrm{U}(\beta_m^{(u)})\,, \quad m \in \{1,\ldots,J\},\ u \in \{1,\ldots,U\}. \qquad (8)$$

Here, $p(b_m^{(u)}|\mathbf{r})$ denotes the conditional probability mass function (pmf) of the information bit $b_m^{(u)}$ given $\mathbf{r}$, $\mathrm{U}(\cdot)$ is the unit

step function, and $\beta_m^{(u)}$ is the posterior log-likelihood ratio (LLR) defined as

$$\beta_m^{(u)} \triangleq \log \frac{p(b_m^{(u)}=1|\mathbf{r})}{p(b_m^{(u)}=0|\mathbf{r})}. \tag{9}$$

In what follows, let $\mathbf{b} \triangleq \big(\mathbf{b}^{(1)T} \cdots \mathbf{b}^{(U)T}\big)^T$ and $\mathbf{c} \triangleq \big(\mathbf{c}^{(1)T} \cdots \mathbf{c}^{(U)T}\big)^T$ denote the vectors containing all information bits and code bits, respectively, of all users; furthermore, let $\mathbf{X} \triangleq (\mathbf{x}^{(1)} \cdots \mathbf{x}^{(U)})$ with $\mathbf{x}^{(u)} \triangleq \big(\mathbf{x}^{(u)T}[1] \cdots \mathbf{x}^{(u)T}[L_x]\big)^T$ be the $M_{\mathrm{T}}L_x \times U$ matrix of all transmit vectors $\mathbf{x}^{(u)}[l]$, $l \in \{1,\ldots,L_x\}$, $u \in \{1,\ldots,U\}$. Similarly, we define the $M_{\mathrm{R}}K \times M_{\mathrm{T}}U$ global channel matrix comprising all MIMO channels $\mathbf{H}^{(u)}[k]$, $k \in \{0,\ldots,K-1\}$, $u \in \{1,\ldots,U\}$ as

$$\mathbf{H} \triangleq \big(\mathbf{H}^{(1)} \cdots \mathbf{H}^{(U)}\big), \quad \text{with } \mathbf{H}^{(u)} \triangleq \big(\mathbf{H}^{(u)T}[0] \cdots \mathbf{H}^{(u)T}[K-1]\big)^T. \tag{10}$$

The posterior bit probabilities $p(b_m^{(u)}|\mathbf{r})$ can be shown to be given by

$$p(b_m^{(u)}|\mathbf{r}) \propto \sum_{\sim b_m^{(u)}} \int p(\mathbf{r},\mathbf{H},\mathbf{X},\mathbf{c}|\mathbf{b})\, d\mathbf{H}.$$

Here and subsequently, the notation $\sum_{\sim b_m^{(u)}}$ denotes summation with respect to *all unobserved* variables in the summand except $b_m^{(u)}$ (in the present case, these variables are $\mathbf{X}$, $\mathbf{c}$, and all elements of $\mathbf{b}$ except $b_m^{(u)}$). Using the facts that $\mathbf{b}$—$\mathbf{c}$—$\mathbf{X}$—$\mathbf{r}$ is a Markov chain and the channel $\mathbf{H}$ is independent of the transmit symbols, the joint pdf $p(\mathbf{r},\mathbf{H},\mathbf{X},\mathbf{c}|\mathbf{b})$ can be further factorized as

$$p(\mathbf{r},\mathbf{H},\mathbf{X},\mathbf{c}|\mathbf{b}) = p(\mathbf{r}|\mathbf{H},\mathbf{X}) \prod_{u=1}^{U} p\big(\mathbf{H}^{(u)}\big)\, p\big(\mathbf{x}^{(u)}|\mathbf{c}^{(u)}\big)\, p\big(\mathbf{c}^{(u)}|\mathbf{b}^{(u)}\big), \tag{11}$$

where we exploited the independence of the channels and of the data of the individual users. This high-level factorization (at the level of vectors and matrices) can be represented by a factor graph as shown in the part of Fig. 3 designated as "High-Level Factor Graph." Note that we use Forney-style factor graphs in the spirit of [19], i.e., factors are represented by boxes (also referred to as "function nodes") and variables are represented by directed edges. (The direction of the edges bears no relevance to the factorization but rather indicates the forward direction of the messages passed in the sum-product algorithm.) We will next refine this factor graph to the level of scalar variables by further factorizing the (conditional) probability density functions (pdfs) and pmfs in (11).

First, the conditional pmf $p\big(\mathbf{c}^{(u)}|\mathbf{b}^{(u)}\big)$ corresponds to the channel encoder and interleaver subsumed by the deterministic mapping $\mathbf{c}^{(u)} = \mathcal{C}^{(u)}(\mathbf{b}^{(u)})$ (cf. (1)); we thus have

$$p\big(\mathbf{c}^{(u)}|\mathbf{b}^{(u)}\big) = \mathrm{I}\big\{\mathbf{c}^{(u)} = \mathcal{C}^{(u)}(\mathbf{b}^{(u)})\big\}. \tag{12}$$

Here, we used the indicator function $\mathrm{I}\{\cdot\}$, which equals 1 if its argument is true and 0 otherwise. The code constraint $\mathrm{I}\big\{\mathbf{c}^{(u)} = \mathcal{C}^{(u)}(\mathbf{b}^{(u)})\big\}$ can be expressed in a more detailed manner by using the code structure, in particular, a trellis/state representation for the convolutional code [17], [18], [21].

Next, the conditional pmf $p\big(\mathbf{x}^{(u)}|\mathbf{c}^{(u)}\big)$ corresponding to the modulator mapping $\mathbf{x}^{(u)}[l] = \chi\big(\mathbf{c}^{(u)}[l]\big)$ reads (cf. (2))

$$p\big(\mathbf{x}^{(u)}|\mathbf{c}^{(u)}\big) = \prod_{i=1}^{M_{\mathrm{T}}} \prod_{l=1}^{L_x} \mathrm{I}\big\{x_i^{(u)}[l] = \chi\big(\mathbf{c}_i^{(u)}[l]\big)\big\}. \tag{13}$$

An example for the refined factor graph portion corresponding to (12) and (13) is shown in Blowup A in Fig. 3.

It remains to provide expressions for $p(\mathbf{H}^{(u)})$ and $p(\mathbf{r}|\mathbf{H},\mathbf{X})$. We will distinguish between the practical case of pilot-aided channel estimation and the "genie" case of perfect CSI (considered for purposes of comparison).

1) Pilot-aided channel estimation: For simplicity, we assume that the MIMO channel elements associated with different antenna pairs are independent; we can then write the channel prior for each user as (cf. (5))

$$p\big(\mathbf{H}^{(u)}\big) = \prod_{i=1}^{M_{\mathrm{T}}} \prod_{j=1}^{M_{\mathrm{R}}} p\big(\mathbf{h}_{j,i}^{(u)}\big), \quad \text{with } p\big(\mathbf{h}_{j,i}^{(u)}\big) = \int \delta\big(\mathbf{h}_{j,i}^{(u)} - \mathbf{F}\tilde{\mathbf{h}}_{j,i}^{(u)}\big)\, p\big(\tilde{\mathbf{h}}_{j,i}^{(u)}\big)\, d\tilde{\mathbf{h}}_{j,i}^{(u)}. \tag{14}$$

Since the distribution of the time-domain channels was assumed to be $\tilde{\mathbf{h}}_{j,i}^{(u)} \sim \mathcal{CN}(\mathbf{0},\mathbf{C}_{\tilde{h}})$ (see Section II-B), the pdf $p\big(\mathbf{h}_{j,i}^{(u)}\big)$ can be explicitly determined as $\mathbf{h}_{j,i}^{(u)} \sim \mathcal{CN}(\mathbf{0},\mathbf{F}\mathbf{C}_{\tilde{h}}\mathbf{F}^H)$. However, from a computational perspective, it is advantageous to stick to the implicit Fourier transform expression (14), whose factor graph representation is shown in Blowup B in Fig. 3 ($\mathcal{F}$ denotes the Fourier transform node).

The channel transfer pdf $p(\mathbf{r}|\mathbf{H},\mathbf{X})$ factorizes into a data part and a pilot part as

$$p(\mathbf{r}|\mathbf{H},\mathbf{X}) = \prod_{j=1}^{M_{\mathrm{R}}} \Bigg[\prod_{k\notin\mathcal{P}} p\big(r_j[k]\big|\mathbf{H}[k],\mathbf{X}[\ell_k]\big)\Bigg] \times \Bigg[\prod_{u=1}^{U}\prod_{i=1}^{M_{\mathrm{T}}}\prod_{k\in\mathcal{P}_i^{(u)}} p\big(r_j[k]\big|\mathbf{h}_i^{(u)}[k]\big)\Bigg], \tag{15}$$

with $r_j[k] \triangleq [\mathbf{r}[k]]_j$, $\mathbf{H}[k] \triangleq \big(\mathbf{H}^{(1)}[k] \cdots \mathbf{H}^{(U)}[k]\big)$, and $\mathbf{X}[l] \triangleq (\mathbf{x}^{(1)}[l] \cdots \mathbf{x}^{(U)}[l])$. The conditional pdfs in (15) can be determined from (6) and (7), respectively:

$$r_j[k]\,\big|\,\mathbf{H}[k],\mathbf{X}[\ell_k] \sim \mathcal{CN}\Bigg(\sum_{u=1}^{U}\sum_{i=1}^{M_{\mathrm{T}}} h_{j,i}^{(u)}[k]\, x_i^{(u)}[\ell_k],\, \sigma_w^2\Bigg), \quad k\notin\mathcal{P},$$

$$r_j[k]\,\big|\,\mathbf{h}_i^{(u)}[k] \sim \mathcal{CN}\big(p h_{j,i}^{(u)}[k],\, \sigma_w^2\big), \quad k\in\mathcal{P}_i^{(u)}.$$

These expressions are the basis for the refined factor graph representation shown in Blowup C in Fig. 3.

2) Perfect CSI: For comparison purposes, it will be useful to consider a genie system with perfect CSI at the receiver, i.e., the receiver knows all channel matrices $\mathbf{H}^{(u)}[k]$ exactly. Since in this case pilot symbols are not needed, we set $K_p = 0$, which implies that $K = L_x$. The factorization of the joint pdf $p(\mathbf{r},\mathbf{H},\mathbf{X},\mathbf{c}|\mathbf{b})$ and the associated factor graph for this case are a simple modification of our previous results; they are obtained by replacing the Gaussian channel distribution in (14) by a point mass at the true channel vector.

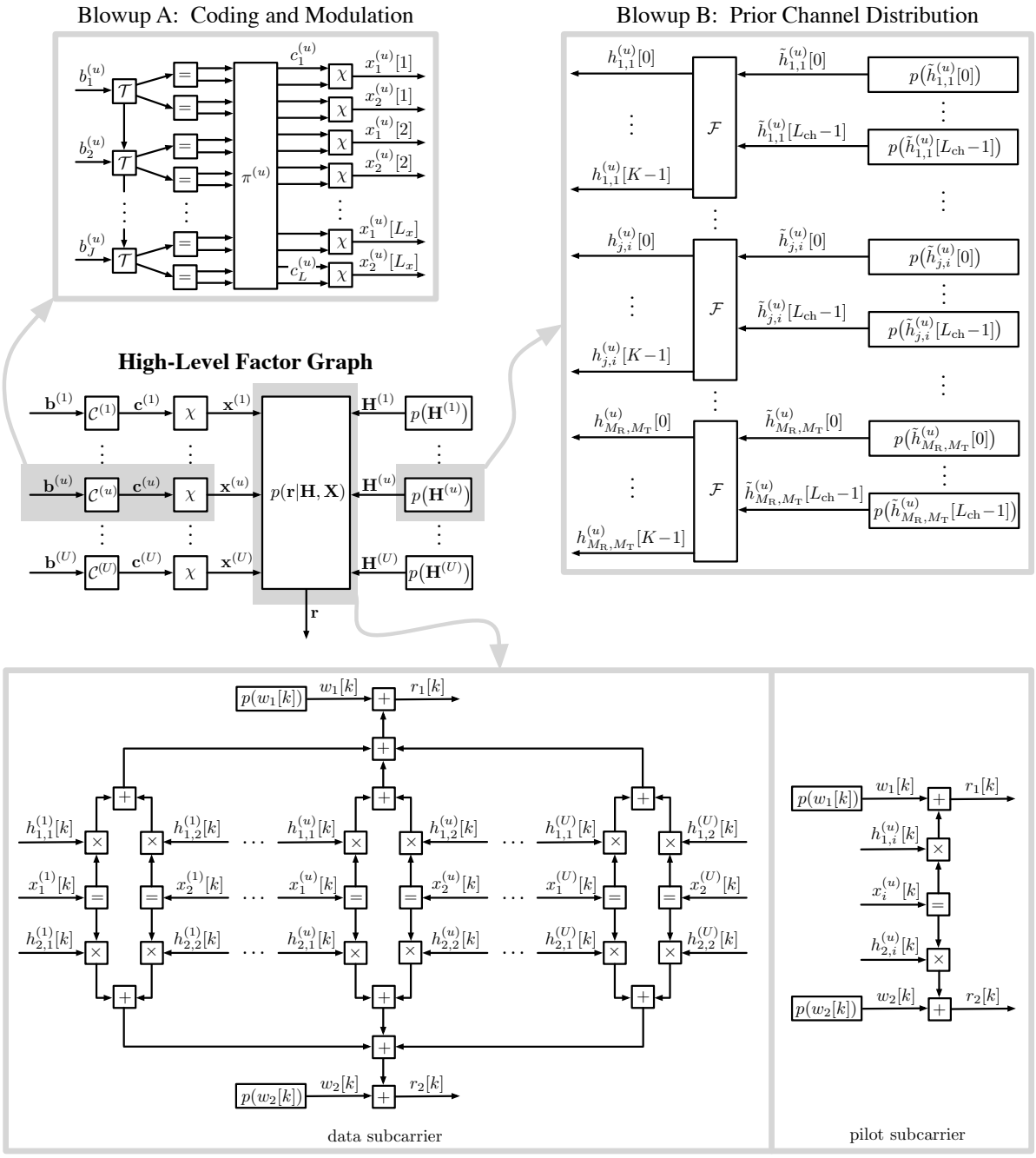

Fig. 3. Forney-style factor graph for a pilot-aided MIMO-OFDM-IDMA system with a rate-1/2 convolutional code (represented by the state-transition nodes labeled $\mathcal{T}$), a rate-1/2 repetition code, 4-QAM modulation, and $M_{\mathrm{T}} = M_{\mathrm{R}} = 2$.

B. Messages

We will next calculate the messages to be propagated along the edges of our factor graph according to the update rules of the sum-product algorithm [18], [19]. Message updates are performed at all nodes with one message per incident edge (variable). These messages are passed in both directions along the directed edges representing the corresponding variable, with forward messages (in the direction of the edge) denoted by $\vec{\mu}(\cdot)$ and backward messages (in the opposite direction of the edge) denoted by $\overleftarrow{\mu}(\cdot)$. For example, in Blowup A in Fig. 3, the message $\vec{\mu}\big(c_1^{(u)}\big)$ is passed from the interleaver node "$\pi^{(u)}$" to a modulator node "χ" along the edge labeled "$c_1^{(u)}$". The following discussion constantly refers to Fig. 3.

We start with the code constraint $\mathrm{I}\big\{\mathbf{c}^{(u)} = \mathcal{C}^{(u)}(\mathbf{b}^{(u)})\big\}$. The sum-product updates for the associated part of the factor graph process the incoming messages $\overleftarrow{\mu}(c_q^{(u)})$ provided by the modulator nodes χ (see below). For decoding, it is advantageous to convert these messages into (*a priori*) LLRs according to

$$\overleftarrow{\xi}_q^{(u)} = \log \frac{\overleftarrow{\mu}\big(c_q^{(u)}=1\big)}{\overleftarrow{\mu}\big(c_q^{(u)}=0\big)} \,.$$

After de-interleaving, as a result of the sum-product algorithm,

the repetition code is decoded by summing up the corresponding LLRs at each repetition node (labeled "=" in Blowup A). This yields the soft inputs for the BCJR decoding algorithm, which soft-decodes the convolutional code using its trellis structure [18], [43]. The BCJR algorithm, which is again an instance of the sum-product algorithm, produces LLRs $\tilde{\beta}_m^{(u)}$ for the information bits and LLRs for the convolutionally encoded bits. The LLRs $\tilde{\beta}_m^{(u)}$ approximate the true posterior LLRs $\beta_m^{(u)}$ in (9) and can be used to obtain tentative bit decisions according to the MAP detection rule (8). The LLRs for the convolutionally encoded bits are passed to the repetition nodes, which compute the sum of all incoming LLRs except the one for which the outgoing LLR is computed. The result of this sum is an "extrinsic" LLR. The extrinsic LLRs are interleaved (the interleaved LLRs will be denoted by $\vec{\xi}_q^{(u)}$) and converted to belief messages according to [19], [20]

$$\vec{\mu}\big(c_q^{(u)}\big) \;=\; \frac{\exp\big(\vec{\xi}_q^{(u)} c_q^{(u)}\big)}{1+\exp\big(\vec{\xi}_q^{(u)}\big)}\,, \qquad c_q^{(u)} \in \{0,1\}\,.$$

These messages are passed on to the modulator nodes χ. The messages $\vec{\mu}\big(x_i^{(u)}[l]\big)$ passed from the modulator nodes χ to the channel transfer node $p(\mathbf{r}|\mathbf{H},\mathbf{X})$ are obtained from the messages $\vec{\mu}\big(c_{\lambda(l,i)+\zeta}\big)$, $\zeta \in \{1,\ldots,B\}$, as (cf. (2))

$$\begin{aligned}\vec{\mu}\big(x_i^{(u)}[l]\big) \;&=\; \sum_{\mathbf{c}_i^{(u)}[l]\in\{0,1\}^B} \mathrm{I}\big\{x_i^{(u)}[l] = \chi\big(\mathbf{c}_i^{(u)}[l]\big)\big\} \\ &\qquad\qquad \times \prod_{\zeta=1}^{B} \vec{\mu}\big(c_{\lambda(l,i)+\zeta}^{(u)}\big) \\ &=\; \bar{\mu}\big(\chi^{-1}\big(x_i^{(u)}[l]\big)\big)\,, \end{aligned} \tag{16}$$

where $\bar{\mu}\big(\mathbf{c}_i^{(u)}[l]\big) \triangleq \prod_{\zeta=1}^{B} \vec{\mu}\big(c_{\lambda(l,i)+\zeta}^{(u)}\big)$. The modulator nodes furthermore perform soft demodulation, which corresponds to the backward messages

$$\begin{aligned}\overleftarrow{\mu}\big(c_{\lambda(l,i)+\zeta}^{(u)}\big) \;&=\; \sum_{\sim c_{\lambda(l,i)+\zeta}^{(u)}} \overleftarrow{\mu}\big(x_i^{(u)}[l]\big)\Big|_{x_i^{(u)}[l]=\chi(\mathbf{c}_i^{(u)}[l])} \\ &\qquad\qquad \times \prod_{\zeta'\neq\zeta} \vec{\mu}\big(c_{\lambda(l,i)+\zeta'}^{(u)}\big)\,. \end{aligned} \tag{17}$$

Expression (17) involves the messages $\overleftarrow{\mu}\big(x_i^{(u)}[\ell_k]\big)$, $k \notin \mathcal{P}$, which are passed from the channel transfer nodes $p(\mathbf{r}[k]|\mathbf{H}[k],\mathbf{X}[\ell_k])$ to the modulator nodes χ. These messages are given by

$$\begin{aligned}\overleftarrow{\mu}\big(x_i^{(u)}[\ell_k]\big) \;&=\; \sum_{\sim x_i^{(u)}[\ell_k]} \int p(\mathbf{r}[k]\,|\mathbf{H}[k],\mathbf{X}[\ell_k])\,\vec{\mu}(\mathbf{H}[k]) \\ &\qquad\qquad \times \frac{\vec{\mu}(\mathbf{X}[\ell_k])}{\vec{\mu}\big(x_i^{(u)}[\ell_k]\big)}\,d\mathbf{H}[k]\,, \quad k\notin\mathcal{P}. \end{aligned} \tag{18}$$

In this expression, $\vec{\mu}(\mathbf{H}[k]) = \prod_{j,i,u} \vec{\mu}\big(h_{j,i}^{(u)}[k]\big)$ and $\vec{\mu}(\mathbf{X}[l]) = \prod_{i,u} \vec{\mu}\big(x_i^{(u)}[l]\big)$ denote the messages sent from the channel state nodes $p\big(\mathbf{H}^{(u)}\big)$ and the (de)modulator nodes χ, respectively, to the channel transfer nodes $p(\mathbf{r}[k]|\mathbf{H}[k],\mathbf{X}[\ell_k])$ (see Section IV); furthermore, the summation is with respect to all elements of $\mathbf{X}[\ell_k]$ except $x_i^{(u)}[\ell_k]$. For the case of perfect CSI at the receiver, $\vec{\mu}(\mathbf{H}[k])$ is a point mass at the true value of the channel and hence (18) simplifies to

$$\begin{aligned}\overleftarrow{\mu}\big(x_i^{(u)}[\ell_k]\big) \;&=\; \sum_{\sim x_i^{(u)}[\ell_k]} p(\mathbf{r}[k]\,|\mathbf{H}[k],\mathbf{X}[\ell_k])\,\frac{\vec{\mu}(\mathbf{X}[\ell_k])}{\vec{\mu}\big(x_i^{(u)}[\ell_k]\big)}\,, \\ &\qquad\qquad k\in\{0,\ldots,K-1\}\,. \end{aligned} \tag{19}$$

Inserting (16) into (18) and, in turn, inserting the result into (17) yields a message update that takes the code bit beliefs $\vec{\mu}\big(c_q^{(u)}\big)$ (equivalently, the extrinsic LLRs $\vec{\xi}_q^{(u)} = \log\frac{\vec{\mu}(c_q^{(u)}=1)}{\vec{\mu}(c_q^{(u)}=0)}$) from the channel decoder and yields improved code bit beliefs $\overleftarrow{\mu}\big(c_q^{(u)}\big)$ (equivalently, improved extrinsic LLRs $\overleftarrow{\xi}_q^{(u)}$). Hence, these message updates taken together can be thought of as a *soft-input/soft-output MIMO multiuser detector*. Since (16) and (17) involve only one antenna of one user, the overall complexity of the MIMO multiuser detector is dominated by (18). In particular, the sum in (18) involves $|\mathcal{S}|^{M_\mathrm{T}U-1}$ terms, so the complexity of calculating $\overleftarrow{\mu}\big(x_i^{(u)}[l]\big)$ is exponential in the number of transmit antennas M_T and in the number of users U. For example, $|\mathcal{S}|^{M_\mathrm{T}U-1} \approx 2.7\cdot 10^8$ for the case of four users, two transmit antennas, and 16-QAM. We note that it is possible to further expand the messages (18) and (19) by using the refined factor graph shown in the left part of Blowup C in Fig. 3. We do not specify these expanded messages since, due to their exponential complexity, we will instead use computationally less expensive approximate messages (to be developed in Section IV).

The channel transfer node $p(\mathbf{r}[k]|\mathbf{H}[k],\mathbf{X}[\ell_k])$ furthermore computes beliefs about the channel coefficients for all data subcarriers:

$$\begin{aligned}\overleftarrow{\mu}\big(h_{j,i}^{(u)}[k]\big) \;&=\; \sum_{\mathbf{X}[\ell_k]\in\mathcal{S}^{M_\mathrm{T}U}} \int p(\mathbf{r}[k]|\mathbf{H}[k],\mathbf{X}[\ell_k])\,\frac{\vec{\mu}\big(\mathbf{H}[k]\big)}{\vec{\mu}\big(h_{j,i}^{(u)}[k]\big)} \\ &\qquad\qquad \times \vec{\mu}\big(\mathbf{X}[\ell_k]\big)\,d{\sim}h_{j,i}^{(u)}[k]\,, \quad k\notin\mathcal{P}_i^{(u)}. \end{aligned} \tag{20}$$

Here, $\int \ldots d{\sim}h_{j,i}^{(u)}[k]$ denotes integration with respect to all elements of $\mathbf{H}[k]$ except $h_{j,i}^{(u)}[k]$. For the pilot subcarriers $k\in\mathcal{P}_i^{(u)}$, the messages for the channel states are given by the Gaussian distribution

$$\overleftarrow{\mu}\big(h_{j,i}^{(u)}[k]\big) \;\propto\; \exp\left(-\frac{\big|h_{j,i}^{(u)}[k]-\frac{r_j[k]}{p}\big|^2}{\frac{\sigma_w^2}{|p|^2}}\right), \quad k\in\mathcal{P}_i^{(u)}. \tag{21}$$

It remains to specify the messages from the channel state nodes to the channel transfer nodes for all data subcarriers. These messages can be obtained from Blowup B as

$$\begin{aligned}\vec{\mu}\big(h_{j,i}^{(u)}[k]\big) \;&=\; \int \delta\big(\mathbf{h}_{j,i}^{(u)} - \mathbf{F}\tilde{\mathbf{h}}_{j,i}^{(u)}\big) \prod_{k'\neq k} \overleftarrow{\mu}\big(h_{j,i}^{(u)}[k']\big) \\ &\qquad\qquad \times \prod_{\nu=0}^{L_\mathrm{ch}-1} \vec{\mu}\big(\tilde{h}_{j,i}^{(u)}[\nu]\big)\,d{\sim}h_{j,i}^{(u)}[k]\,, \quad k\notin\mathcal{P}. \end{aligned} \tag{22}$$

The messages $\vec{\mu}\big(h_{j,i}^{(u)}[\nu]\big)$ involved in this expression will be discussed in Section IV-A2.

IV. Low-Complexity Receiver

In general, the message updates (18), (20), and (22) are too computationally complex for practical implementations. Therefore, we next discuss two modifications of our iterative receiver that yield a significant reduction of computational complexity. First, we use Gaussian approximations for the symbol and channel messages, so that closed-form integration can be used to simplify the message updates. For Gaussian messages, it suffices to update and pass the mean and (co)variance [19]; the corresponding (forward and backward) messages will be denoted by $\vec{m}(\cdot)$, $\overleftarrow{m}(\cdot)$, $\vec{\sigma}(\cdot)$, and $\overleftarrow{\sigma}(\cdot)$. The complexity of the multiuser detector resulting from the Gaussian approximations is only linear in the number of users, instead of exponential. The second modification we propose achieves an additional complexity reduction by updating only a subset of the messages; this subset is selected dynamically during each iteration.

To justify the approach taken in this section, we note that joint channel estimation and decoding is still far from being fully understood. Several approaches have been proposed in the literature based on expectation-maximization [26], variational message passing [29], and Gaussian approximations [24], [27]. However, the overall receiver performance depends also on the interplay with the equalizer employed and on the quality of the initial channel estimates. Hence, currently no general statement as to which scheme is preferable can be made. Therefore, we stick to standard sum-product updates with Gaussian approximations. Integrating channel estimation into the message passing receiver creates numerous additional cycles in the factor graph. In our framework, this problem is mitigated by scheduling the updates of the channel messages at later iterations and by performing selective message updates.

A. Gaussian Approximations

1) Channel transfer node: To simplify the calculation of $\overleftarrow{\mu}\big(x_i^{(u)}[l]\big)$ in (18) (alternatively, in (19)), we approximate the beliefs $\vec{\mu}\big(x_i^{(u)}[l]\big)$ in (16) by Gaussian distributions with the same means and variances as those of the true beliefs. Using (16), these means and variances are obtained as

$$\vec{m}\big(x_i^{(u)}[l]\big) = \sum_{x_i^{(u)}[l]\in\mathcal{S}} x_i^{(u)}[l]\,\bar{\mu}\big(\chi^{-1}\big(x_i^{(u)}[l]\big)\big),$$

$$\vec{\sigma}\big(x_i^{(u)}[l]\big) = \sum_{x_i^{(u)}[l]\in\mathcal{S}} \big|x_i^{(u)}[l] - \vec{m}\big(x_i^{(u)}[l]\big)\big|^2\,\bar{\mu}\big(\chi^{-1}\big(x_i^{(u)}[l]\big)\big).$$

Furthermore, we also approximate the beliefs $\vec{\mu}\big(h_{j,i}^{(u)}[k]\big)$ by Gaussians with means $\vec{m}\big(h_{j,i}^{(u)}[k]\big)$ and variances $\vec{\sigma}\big(h_{j,i}^{(u)}[k]\big)$, which will be determined at the end of this subsection. For what follows, we define $\vec{\mathbf{m}}\big(\mathbf{h}_i^{(u)}[k]\big) \triangleq \big(\vec{m}\big(h_{1,i}^{(u)}[k]\big)\cdots \vec{m}\big(h_{M_\mathrm{R},i}^{(u)}[k]\big)\big)^T$, $\vec{\mathbf{C}}\big(\mathbf{h}_i^{(u)}[k]\big) \triangleq \operatorname{diag}\big\{\vec{\sigma}\big(h_{1,i}^{(u)}[k]\big),\ldots,\vec{\sigma}\big(h_{M_\mathrm{R},i}^{(u)}[k]\big)\big\}$, and $\mathcal{G}(\mathbf{x},\mathbf{C}) \triangleq \exp(-\mathbf{x}^H\mathbf{C}^{-1}\mathbf{x})$. Using the Gaussian approximations for the forward messages $\vec{\mu}\big(x_i^{(u)}[l]\big)$ and $\vec{\mu}\big(\mathbf{h}_i^{(u)}[k]\big) = \prod_{j=1}^{M_\mathrm{R}} \vec{\mu}\big(h_{j,i}^{(u)}[k]\big)$, the corresponding Gaussian approximations for the backward messages $\overleftarrow{\mu}\big(x_i^{(u)}[l]\big)$ can be evaluated for $k\notin\mathcal{P}$ as [19]

$$\overleftarrow{\mu}\big(x_i^{(u)}[\ell_k]\big) \propto \mathcal{G}\Big(x_i^{(u)}[\ell_k]\,\vec{\mathbf{m}}\big(\mathbf{h}_i^{(u)}[k]\big) - \mathbf{m}_i^{(u)}[k]\,,\,\mathbf{C}_i^{(u)}[k]\Big). \tag{23}$$

Here, the mean vector $\mathbf{m}_i^{(u)}[k]$ and covariance matrix $\mathbf{C}_i^{(u)}[k]$ are given by

$$\mathbf{m}_i^{(u)}[k] = \mathbf{r}[k] - \sum_{(i',u')\neq(i,u)} \vec{m}\big(x_{i'}^{(u')}[\ell_k]\big)\,\vec{\mathbf{m}}\big(\mathbf{h}_{i'}^{(u')}[k]\big),$$

$$\mathbf{C}_i^{(u)}[k] = \big|x_i^{(u)}[\ell_k]\big|^2\,\vec{\mathbf{C}}\big(\mathbf{h}_i^{(u)}[k]\big) + \widetilde{\mathbf{C}}_i^{(u)}[k] + \sigma_w^2\mathbf{I},$$

where

$$\widetilde{\mathbf{C}}_i^{(u)}[k] = \sum_{(i',u')\neq(i,u)} \Big[\vec{\sigma}\big(x_{i'}^{(u')}[\ell_k]\big)\,\vec{\mathbf{m}}\big(\mathbf{h}_{i'}^{(u')}[k]\big)\,\vec{\mathbf{m}}^H\big(\mathbf{h}_{i'}^{(u')}[k]\big) + \Big(\big|\vec{m}\big(x_{i'}^{(u')}[\ell_k]\big)\big|^2 + \vec{\sigma}\big(x_{i'}^{(u')}[\ell_k]\big)\Big)\vec{\mathbf{C}}\big(\mathbf{h}_{i'}^{(u')}[k]\big)\Big].$$

The overall complexity of (approximately) calculating $\overleftarrow{\mu}\big(x_i^{(u)}[l]\big)$ can be shown to scale linearly with the number of users U and cubically with the number of transmit antennas M_T. We note that for the case of perfect CSI, the message $\overleftarrow{\mu}\big(x_i^{(u)}[\ell_k]\big)$ is obtained according to (23) with $\vec{\mathbf{m}}\big(\mathbf{h}_i^{(u)}[k]\big) = \mathbf{h}_i^{(u)}[k]$ and $\vec{\mathbf{C}}\big(\mathbf{h}_i^{(u)}[k]\big) = \mathbf{0}$.

In a similar manner, the messages $\overleftarrow{\mu}\big(\mathbf{h}_i^{(u)}[k]\big)$ in (20) can be approximated as

$$\overleftarrow{\mu}\big(\mathbf{h}_i^{(u)}[k]\big) \propto \mathcal{G}\left(\mathbf{h}_i^{(u)}[k] - \overleftarrow{\mathbf{m}}\big(\mathbf{h}_i^{(u)}[k]\big)\,,\,\frac{\overleftarrow{\mathbf{C}}\big(\mathbf{h}_i^{(u)}[k]\big)}{\big|\vec{m}\big(x_i^{(u)}[\ell_k]\big)\big|^2}\right),\quad k\notin\mathcal{P}_i^{(u)}, \tag{24}$$

with mean and covariance

$$\overleftarrow{\mathbf{m}}\big(\mathbf{h}_i^{(u)}[k]\big) = \frac{\mathbf{m}_i^{(u)}[k]}{\vec{m}(x_i^{(u)}[\ell_k])},\quad \overleftarrow{\mathbf{C}}\big(\mathbf{h}_i^{(u)}[k]\big) = \widetilde{\mathbf{C}}_i^{(u)}[k] + \sigma_w^2\mathbf{I}.$$

2) Channel state node: We next consider the (approximate) calculation of the messages $\vec{\mu}\big(\mathbf{h}_{j,i}^{(u)}\big) = \prod_{k=0}^{K-1}\vec{\mu}\big(h_{j,i}^{(u)}[k]\big)$. Using the Gaussianity of the messages in (21) and the Gaussian approximation (24) for the messages $\overleftarrow{\mu}\big(\mathbf{h}_i^{(u)}[k]\big)$, it follows that $\overleftarrow{\mu}\big(\mathbf{h}_{j,i}^{(u)}\big) = \prod_{k=0}^{K-1}\overleftarrow{\mu}\big(h_{j,i}^{(u)}[k]\big)$ is Gaussian with mean vector $\overleftarrow{\mathbf{m}}\big(\mathbf{h}_{j,i}^{(u)}\big)$ and diagonal covariance matrix $\overleftarrow{\mathbf{C}}\big(\mathbf{h}_{j,i}^{(u)}\big)$ given by

$$\big[\overleftarrow{\mathbf{m}}\big(\mathbf{h}_{j,i}^{(u)}\big)\big]_k = \begin{cases}[\mathbf{r}[k]]_j/p\,, & k\in\mathcal{P}_i^{(u)}\\ \big[\overleftarrow{\mathbf{m}}\big(\mathbf{h}_i^{(u)}[k]\big)\big]_j\,, & k\notin\mathcal{P}_i^{(u)},\end{cases}$$

$$\big[\overleftarrow{\mathbf{C}}\big(\mathbf{h}_{j,i}^{(u)}\big)\big]_{k,k} = \begin{cases}\sigma_w^2/|p|^2\,, & k\in\mathcal{P}_i^{(u)}\\ \big[\overleftarrow{\mathbf{C}}\big(\mathbf{h}_i^{(u)}[k]\big)\big]_{j,j}\,, & k\notin\mathcal{P}_i^{(u)}.\end{cases}$$

Due to the Fourier transform relation $\tilde{\mathbf{h}}_{j,i}^{(u)} = \mathbf{F}^H\mathbf{h}_{j,i}^{(u)}$ (cf. (5)), we have $\overleftarrow{\mathbf{m}}\big(\tilde{\mathbf{h}}_{j,i}^{(u)}\big) = \mathbf{F}^H\overleftarrow{\mathbf{m}}\big(\mathbf{h}_{j,i}^{(u)}\big)$ and $\overleftarrow{\mathbf{C}}\big(\tilde{\mathbf{h}}_{j,i}^{(u)}\big) = \mathbf{F}^H\overleftarrow{\mathbf{C}}\big(\mathbf{h}_{j,i}^{(u)}\big)\mathbf{F}$. Multiplying in the Gaussian prior $\mathcal{CN}(\mathbf{0},\mathbf{C}_{\tilde{\mathbf{h}}})$ results in the forward messages

$$\vec{\mathbf{m}}\big(\tilde{\mathbf{h}}_{j,i}^{(u)}\big) \;=\; \vec{\mathbf{C}}\big(\tilde{\mathbf{h}}_{j,i}^{(u)}\big)\,\overleftarrow{\mathbf{C}}^{-1}\big(\tilde{\mathbf{h}}_{j,i}^{(u)}\big)\,\overleftarrow{\mathbf{m}}\big(\tilde{\mathbf{h}}_{j,i}^{(u)}\big)\,,$$
$$\vec{\mathbf{C}}\big(\tilde{\mathbf{h}}_{j,i}^{(u)}\big) \;=\; \Big(\overleftarrow{\mathbf{C}}^{-1}\big(\tilde{\mathbf{h}}_{j,i}^{(u)}\big) + \mathbf{C}_{\tilde{\mathbf{h}}}^{-1}\Big)^{-1}.$$

Again invoking the Fourier transform relation (5) yields the subcarrier-domain forward messages

$$\vec{\mathbf{m}}\big(\mathbf{h}_{j,i}^{(u)}\big) = \mathbf{F}\,\vec{\mathbf{m}}\big(\tilde{\mathbf{h}}_{j,i}^{(u)}\big)\,, \quad \vec{\mathbf{C}}\big(\mathbf{h}_{j,i}^{(u)}\big) = \mathbf{F}\,\vec{\mathbf{C}}\big(\tilde{\mathbf{h}}_{j,i}^{(u)}\big)\,\mathbf{F}^{H}.$$

The elements $\vec{m}\big(h_{j,i}^{(u)}[k]\big) = \big[\vec{\mathbf{m}}\big(\mathbf{h}_{j,i}^{(u)}\big)\big]_k$ and $\vec{\sigma}\big(h_{j,i}^{(u)}[k]\big) = \big[\vec{\mathbf{C}}\big(\mathbf{h}_{j,i}^{(u)}\big)\big]_{k,k}$ were considered at the beginning of this subsection.

During the initial iterations of the sum-product algorithm, we observed the channel "estimates" $\big[\overleftarrow{\mathbf{m}}\big(\mathbf{h}_{j,i}^{(u)}\big)\big]_k$ in the backward direction to be unreliable at non-pilot subcarriers (i.e., for $k \notin \mathcal{P}_i^{(u)}$, the associated variances were very large). Therefore, during a certain number of initial iterations, we set $\big[\overleftarrow{\mathbf{m}}\big(\mathbf{h}_{j,i}^{(u)}\big)\big]_k = 0$ and $\big[\overleftarrow{\mathbf{C}}\big(\mathbf{h}_{j,i}^{(u)}\big)\big]_{k,k} = 0$ for $k \notin \mathcal{P}_i^{(u)}$.

B. Selective Message Update

The calculation (update) of the messages $\overleftarrow{\mu}\big(c_q^{(u)}\big)$ can be very costly, even when the Gaussian approximations developed in the previous subsection are used. We therefore propose a scheme that achieves a reduction of the number of updates by calculating updated beliefs only for code bits with poor reliability. The reliability of a code bit $c_q^{(u)}$ is measured by its posterior LLR, which is given by [18]–[20]

$$\xi_q^{(u)} \;=\; \overrightarrow{\xi}_q^{(u)} + \overleftarrow{\xi}_q^{(u)}. \tag{25}$$

If $\big|\xi_q^{(u)}\big|$ exceeds a prescribed threshold, the soft estimate $\xi_q^{(u)}$ of the code bit $c_q^{(u)}$ is qualified as reliable and the corresponding message $\overleftarrow{\mu}\big(c_q^{(u)}\big)$ is no longer updated, i.e., the value from the previous iteration is reused (note that the LLR threshold may change during the iterations). In the course of the iterations of the sum-product algorithm, the code bit reliabilities improve and hence fewer and fewer message updates have to be performed. This *selective message update* can be viewed as an adaptive message-update schedule [17] of the sum-product algorithm that dynamically adapts to the current bit reliabilities (i.e., which code bit LLRs are updated when and how often depends on the specific channel and noise realization).

The choice of the threshold affects both the number of message updates that have to be carried out—this number decreases with decreasing threshold—and the performance of the sum-product algorithm (convergence behavior and final BER). Since the LLRs generally increase with the SNR, the threshold has to be adapted to the SNR. The impact of the LLR threshold on the performance and complexity of the receiver will be studied experimentally in Section VI. Our experimental results indicate that the proposed selective message update scheme incurs only a small performance loss or, in some cases, even improves the performance (i.e., decreases the BER). These observations support the use of (25) as a reliability measure.

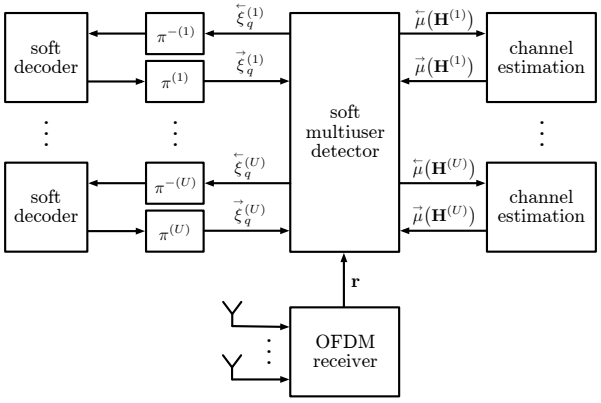

Fig. 4. Overall structure of the proposed MIMO-OFDM-IDMA receiver performing joint detection and channel estimation (cf. the part of Fig. 3 labeled "High-Level Factor Graph"). The de-interleaver of user u is denoted by $\pi^{-(u)}$.

The number of messages updated per iteration depends on the LLR threshold and on system parameters like SNR, number of users, number of antennas, and symbol constellation. For practical implementations in hardware, it is sometimes desirable to prescribe the complexity per iteration. This can be easily achieved by updating only a fixed number $L_0 \leq UL$ of messages $\overleftarrow{\mu}\big(c_q^{(u)}\big)$, namely those that correspond to the L_0 posterior LLRs $\xi_q^{(u)}$ with smallest magnitude. Such an approach can be viewed as a selective message update scheme in which the LLR threshold is chosen such that L_0 posterior LLR magnitudes lie below the threshold. A smaller receiver complexity is obtained by choosing a smaller value of L_0. Thus, the complexity of this method is controlled by choosing L_0 or, equivalently, the fraction $\alpha = L_0/(UL)$ of code bit message updates. The chosen L_0 may vary in the course of the iterations; this is useful since typically the number of posterior LLRs with small magnitude decreases with increasing number of iterations. Since the complexity per iteration and the total complexity of this scheme can be fixed in advance, we refer to this variant of selective message updating as "fixed-complexity" scheme.

C. Overall Receiver Structure

The message-passing algorithm developed above can be interpreted as an iterative turbo receiver structure as shown in Fig. 4. The "OFDM receiver" stage removes the cyclic prefix and calculates the frequency-domain sequence $\mathbf{r}$ by means of a DFT. The box labeled "soft multiuser detector" represents a soft-input/soft-output MIMO multiuser detector, which exchanges messages with the U nodes of the code constraints $\mathrm{I}\big\{\mathbf{c}^{(u)} = \mathcal{C}^{(u)}(\mathbf{b}^{(u)})\big\}$ (located in Blowup A in Fig. 3). The U parallel single-user "soft decoders" shown in Fig. 4 correspond to the code constraint nodes of Fig. 3. The soft multiuser detector also exchanges messages with the box denoted "channel estimation."

More specifically, the multiuser detector takes the extrinsic code bit LLRs $\overrightarrow{\xi}_q^{(u)}$ produced by the channel decoders as input and passes refined code bit LLRs $\overleftarrow{\xi}_q^{(u)}$ back to the channel decoders. The proposed receiver uses parallel message

scheduling [17], i.e., the extrinsic LLRs $\vec{\xi}_q^{(u)}$ for all users at the input of the multiuser detector are simultaneously updated by the channel decoders, and then used by the multiuser detector to calculate refined messages for all users concurrently. We note that the multiuser detector corresponds to the sum-product algorithm operating on the factor graph in Blowup C augmented by the modulation nodes in Blowup A (see Fig. 3). In a similar manner, the messages $\vec{\mu}(\mathbf{H}^{(u)})$ obtained from the multiuser detector are used by the channel estimation block to calculate refined estimates $\overleftarrow{\mu}(\mathbf{H}^{(u)})$ of the channel coefficients, which are used in the next iteration. The channel estimation block corresponds to the sum-product algorithm operating on the factor graph in Blowup B.

When the message-passing algorithm is terminated after a predefined number of iterations, the signs of the posterior LLRs $\tilde{\beta}_m^{(u)}$ of the information bits calculated by the BCJR channel decoder provide the final bit decisions approximating (8).

V. Achievable Rates of IDMA

In Section VI, we will illustrate the BER performance of the proposed low-complexity MIMO-OFDM-IDMA receiver derived in Section IV (without selective message update). These BER results depend on the specific channel code used. Therefore, in this section, we consider the information rates achievable with our scheme (excluding the channel code) as an alternative, code-independent performance metric. More specifically, we compare the achievable rate of the IDMA receiver with the information-theoretic capacity of the underlying multiple-access channel (MAC). We restrict our discussion to the case of perfect receive CSI and no transmit CSI.

The (ergodic) sum-rate of the MAC (6) is given by (cf. [44])

$$R_{\mathrm{s}} = \sum_{u=1}^{U} R_u = I(\mathbf{X};\mathbf{r})\,,$$

where R_u denotes the individual rate of the uth user and $I(\mathbf{X};\mathbf{r})$ is the mutual information given by

$$I(\mathbf{X};\mathbf{r}) = \mathrm{E}\left\{ \log_2 \frac{2^{UM_{\mathrm{T}}B}\, p(\mathbf{r}|\mathbf{H},\mathbf{X})}{\sum_{\mathbf{X}'} p(\mathbf{r}|\mathbf{H},\mathbf{X}')} \right\}. \qquad (26)$$

Here, $p(\mathbf{r}|\mathbf{H},\mathbf{X})$ is the channel transfer pdf specified in (15) and the expectation is with respect to $\mathbf{r}$, $\mathbf{H}$, and $\mathbf{X}$. We assume a symmetric MAC with identical user rates $R_u = R_{\mathrm{s}}/U$.

We first consider a single-antenna OFDM-IDMA system (i.e., $M_{\mathrm{T}} = M_{\mathrm{R}} = 1$) with $U = 4$ users and BPSK modulation. For this setup, Fig. 5 shows (i) the normalized information-theoretic sum rate $R_u = I(\mathbf{X};\mathbf{r})/U$ versus the SNR (defined as the mean symbol energy $\mathrm{E}\{|x_i^{(u)}[l]|^2\}$ divided by the noise variance σ_w^2) and (ii) the SNR thresholds (defined below) of the low-complexity IDMA receiver of Section IV for code rates R of 0.1, 0.125, and 0.2 bits per channel use (bpcu). In order to determine the ergodic sum-rate of the MAC, we estimated $I(\mathbf{X};\mathbf{r})$ in (26) by means of Monte Carlo simulation. For the rate achievable with the low-complexity IDMA receiver, a closed-form expression is not available. Therefore, to obtain estimates of that rate, we performed BER simulations

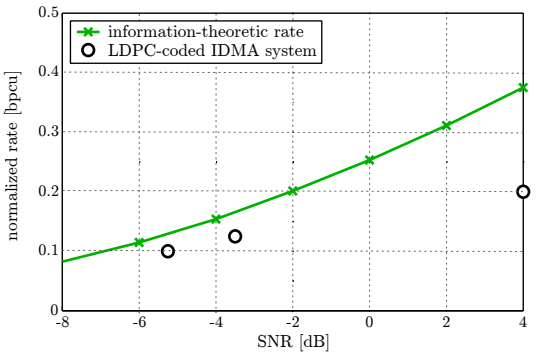

Fig. 5. Achievable rates for a single-antenna MAC with four users and BPSK modulation: information-theoretic normalized (per user) sum-rate ('×') and three operating points of an LDPC-coded IDMA system ('○').

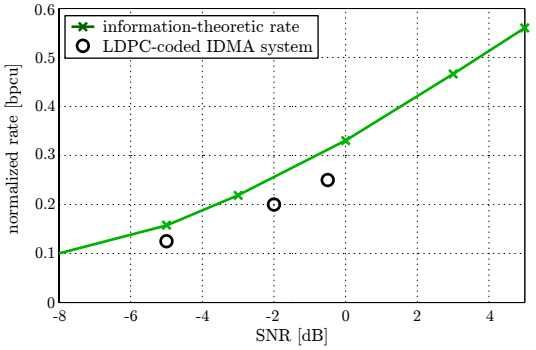

Fig. 6. Achievable rates for a 2×2 MIMO-MAC with two users and BPSK modulation: information-theoretic normalized (per user) sum-rate ('×') and three operating points of an LDPC-coded MIMO-IDMA system ('○').

using LDPC codes[2] [45] instead of the concatenation of convolutional and repetition codes described in Section II. Because of the strong performance of LDPC codes, the BER waterfall region of the IDMA receiver is close to the SNR threshold of the IDMA system at the rate corresponding to the LDPC code. The SNR thresholds above which the BER is below 10^{-4} are shown as operating points in Fig. 5. It can be seen that for code rates of $R = 0.1$ bpcu and $R = 0.125$ bpcu, the proposed low-complexity IDMA system performs about 2 dB away from the information-theoretic limit. For a code rate of $R = 0.2$ bpcu, we observe a much larger gap of about 6 dB. This gap can be attributed to the fact that at higher SNR/higher rate, there is a mismatch between the AWGN channel assumed for the LDPC code design and the multi-access interference in the IDMA system.

Fig. 6 shows results for a 2×2 MIMO-OFDM-IDMA system with two users and BPSK modulation. The code rate R for the LDPC-coded BER simulations was chosen as 0.125, 0.2, and 0.25 bpcu. It is seen that for all three rates, the SNR thresholds above which the BER is below 10^{-4} lie within 2 dB of the information-theoretic limit.

VI. Simulation Results

In this section, we present simulation results for the proposed MIMO-OFDM-IDMA receivers. We will first consider

[2]The LDPC code was designed using the EPFL web-tool at `http://lthcwww.epfl.ch/research/ldpcopt`.

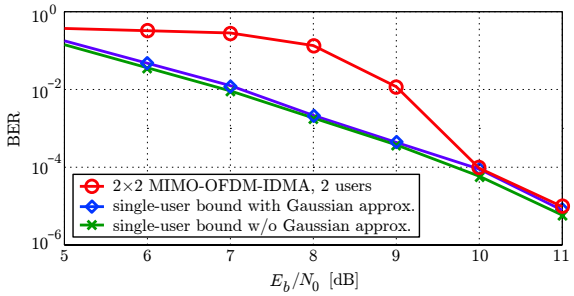

Fig. 7. BER versus SNR E_b/N_0 achieved by the proposed low-complexity MIMO-OFDM-IDMA receiver with perfect CSI ($M_{\mathrm{T}} = M_{\mathrm{R}} = 2$, $U = 2$, 16-QAM). Single-user bounds are shown as performance benchmarks.

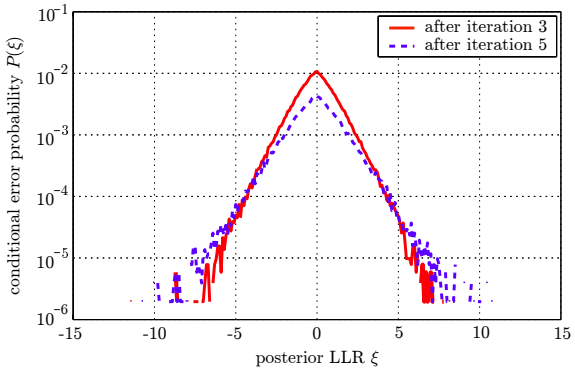

Fig. 8. Empirical conditional code bit error probability $P(\xi)$ given that the posterior LLR is approximately equal to ξ ($M_{\mathrm{T}} = M_{\mathrm{R}} = 2$, $U = 2$, 16-QAM).

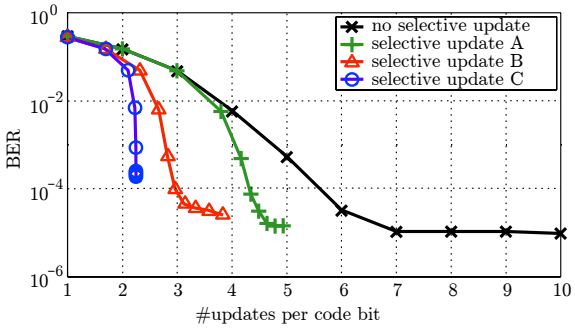

Fig. 9. BER versus average number of message updates per code bit for different selective message update schemes and for the receiver without selective message updates ($M_{\mathrm{T}} = M_{\mathrm{R}} = 2$, $U = 2$, 16-QAM, $E_b/N_0 = 11$ dB).

receivers with perfect CSI and justify the selective message update scheme. Then, we will study pilot-aided receivers performing joint multiuser data detection and channel estimation. In all simulations, static frequency-selective channels are considered; furthermore, the channel code is a serial concatenation of a terminated convolutional code with rate $R_1 = 1/2$ and code polynomial $[23\ 35]_8$ and a repetition code with rate $R_2 = 1/U$. The overall code rate of each user thus equals $R = 1/(2U)$. The interleavers were generated randomly for each user. All receivers performed ten message-passing iterations unless stated otherwise.

A. Receivers with Perfect CSI

We first consider various versions of the genie-aided receiver with perfect CSI. We simulated a 2×2 MIMO-OFDM-IDMA system with $U = 2$ users, a packet size of $L = 2048$ code bits (i.e., $J = RL = 512$ information bits), and 16-QAM modulation. For both users, the matrix impulse response of the frequency-selective MIMO channel comprises $L_{\mathrm{ch}} = 40$ i.i.d. taps, each with i.i.d. standard normal matrix elements. Unless stated otherwise, we consider the low-complexity receiver based on Gaussian approximations.

1) No selective message updates: Fig. 7 shows the BER versus the SNR[3] E_b/N_0 after ten message-passing iterations (due to symmetry, both users have the same BER). For comparison, we also show two single-user bounds, i.e., the BER achieved for the case of only one user without and with the Gaussian approximation. It is seen that these single-user bounds are very close to each other, thereby justifying the Gaussian approximation. We furthermore observe that for an SNR of $E_b/N_0 > 10$ dB, the two-user system performs close to the single-user bounds. This shows that multi-access interference is almost completely suppressed by our low-complexity receiver.

2) Selective message updates: Next, we use the selective message update scheme of Subsection IV-B in our low-complexity receiver. We first present simulation results justifying the selective message update scheme. To this end, we determined detected code bits $\hat{c}_q^{(u)} = \mathrm{U}\big(\xi_q^{(u)}\big)$ based on the sign of the associated posterior LLR $\xi_q^{(u)}$ (see (25)). We are specifically interested in the code bit error probability conditioned on the posterior LLR, i.e., $P(\xi) \triangleq P\big\{\hat{c}_q^{(u)} \neq c_q^{(u)} \,\big|\, \xi_q^{(u)} = \xi\big\}$. We approximated this probability by empirical estimates of the conditional error probability given that the posterior LLR lies in a small interval about a prescribed posterior LLR ξ, i.e., $P(\xi) \approx P\big\{\hat{c}_q^{(u)} \neq c_q^{(u)} \,\big|\, |\xi_q^{(u)} - \xi| \leq 0.05\big\}$. Fig. 8 shows the results for $M_{\mathrm{T}} = M_{\mathrm{R}} = 2$, $U = 2$, and 16-QAM, after three iterations and after five iterations. It can be seen that posterior LLRs with large magnitude indeed lead to a low conditional error probability. This experimental result justifies the idea of not updating the message $\overleftarrow{\mu}\big(c_q^{(u)}\big)$ when $\big|\xi_q^{(u)}\big|$ exceeds a certain threshold.

In Fig. 9, we study the BER-versus-complexity performance of the low-complexity receiver, both with and without selective message updates, at an SNR of $E_b/N_0 = 11$ dB. The complexity measure considered is the average number of message updates per code bit, i.e., the total number of updates of the messages $\overleftarrow{\mu}\big(c_q^{(u)}\big)$ normalized by the codeword length L and the number of users U (without selective updates, this is equivalent to the number of iterations). We compare three selective update schemes with different choices of the LLR threshold. Schemes A and C use a constant LLR threshold of 30 and 5, respectively. Hence, scheme C performs fewer updates than scheme A. Scheme B uses an LLR threshold that increases linearly from 5 (first iteration) to 30 (tenth iteration); this is motivated by the fact that the LLR magnitude tends to increase in the course of the iterations. From Fig. 9, we can draw the

[3]The SNR E_b/N_0 involves the energy per bit E_b, i.e., the total transmit energy for data and pilots normalized by the number of information bits, which is given by $E_b = K\,\mathrm{E}\big\{\big|x_i^{(u)}[l]\big|^2\big\}/J$.

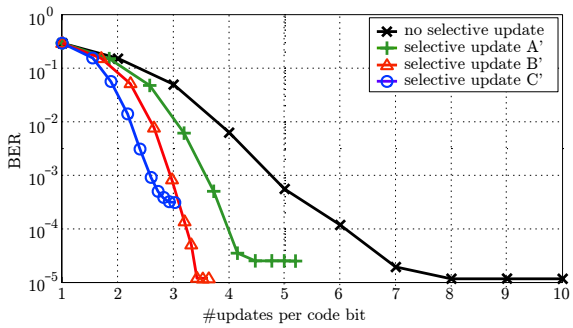

Fig. 10. BER versus average number of message updates per code bit for different fixed-complexity selective message update schemes and for the receiver without selective message updates ($M_{\mathrm{T}} = M_{\mathrm{R}} = 2$, $U = 2$, 16-QAM, $E_b/N_0 = 11$ dB).

general conclusion that the selective message update strategy offers a very favorable performance-complexity tradeoff. The receiver without selective message updates is seen to have the slowest BER decrease for a growing number of updates; after seven iterations (equivalently, seven message updates per code bit), it saturates at a BER close to 10^{-5}. Scheme C exhibits the quickest BER decrease and saturates at a BER slightly above 10^{-4} and a complexity of about 2.2 updates per code bit; no more updates are performed after that point. The last iterations reduce the BER only slightly but at the same time require only very few updates since most posterior LLR magnitudes are already larger than 5. The behavior of scheme A initially equals that observed without selective updates. Eventually, however, LLR thresholding sets in and the further BER decrease (down to slightly above 10^{-5}) is achieved with significantly less complexity than without selective updates. The results of scheme B are intermediate between those of schemes A and C, with a quick initial BER decrease and saturation at a reasonably low BER. To achieve a target BER of 10^{-4} (or better), the method without selective updates requires six message updates per code bit whereas scheme B requires (on average) only three updates per code bit, corresponding to computational savings of about 50%. Furthermore, after (on average) three message updates per code bit, the BER of scheme B is almost three orders of magnitude lower than that of the receiver without selective updates.

3) Fixed-complexity message updates: We next consider three selective message update schemes with fixed complexity, i.e., performing a prescribed number of updates per iteration. These schemes, which are denoted A′, B′, and C′, all update a fraction α of messages that decreases in the course of the iterations; in each iteration, we have $\alpha_{\mathrm{A}'} \geq \alpha_{\mathrm{B}'} \geq \alpha_{\mathrm{C}'}$. Fig. 10 shows the BER versus complexity (average number of updates per code bit) for the three schemes and for the receiver without selective updates, again at an SNR of $E_b/N_0 = 11$ dB. The conclusions are essentially the same as before. Scheme C′ is computationally the most efficient among the three schemes but saturates at a BER of about $3 \cdot 10^{-4}$. For a target BER close to 10^{-5}, scheme B′ leads to computational savings of almost 60% relative to the receiver without selective updates. Scheme A′ is again more complex than scheme B′; interestingly, it has also a higher saturation BER.

In Fig. 11, we consider a near-far scenario in which the receive SNR of the first user is 3 dB higher than that of the second user. We compare three different update schemes $\tilde{\mathrm{A}}$, $\tilde{\mathrm{B}}$, and $\tilde{\mathrm{C}}$, all of which use the same total number of message updates per iteration, which decreases in the course of the iterations. With scheme $\tilde{\mathrm{A}}$, the number of updates per iteration is evenly split among the two users; scheme $\tilde{\mathrm{B}}$ assigns more updates to user #1; and scheme $\tilde{\mathrm{C}}$ assigns more updates to user #2. Fig. 11 shows the BER-versus-complexity curves for the three schemes and for the receiver without selective updates. It is seen that the BER of user #1 is lower than that of user #2 by up to almost two orders of magnitude. However, for both users, the BER performance after ten iterations is best with scheme $\tilde{\mathrm{C}}$ and worst with scheme $\tilde{\mathrm{B}}$ (scheme $\tilde{\mathrm{A}}$ performs in between). This is intuitive because the limited number of updates are better spent on the code bit LLRs of user #2, which are generally smaller than those of user #1 due to the lower receive SNR of user #2.

B. Receivers Performing Joint Channel Estimation and Data Detection

Next, we present results for the case where the channel needs to be estimated using pilots. Throughout this section, we consider (i) the proposed receiver performing joint data detection and pilot-aided channel estimation (with or without selective updates); (ii) a conventional receiver that first estimates the channel coefficients by means of a pilot-aided MMSE estimator and then uses the channel estimates for iterative data detection; and (iii) the genie-aided receiver with perfect CSI. In the proposed receiver, the messages $\overleftarrow{\mu}(\mathbf{H}^{(u)})$ were used for refining the channel estimate messages $\overrightarrow{\mu}(\mathbf{H}^{(u)})$ only after the second iteration unless indicated otherwise.

1) Single-antenna system: We first consider the single-input single-output (SISO) case, i.e., $M_{\mathrm{T}} = M_{\mathrm{R}} = 1$. We simulated a pilot-aided SISO-OFDM-IDMA system with $U = 4$ users, each transmitting $L_x = 2048$ BPSK symbols, corresponding to $J = 256$ information bits. We used $K = 2276$ OFDM subcarriers so that each user transmits $K_p = (K - L_x)/U = 57$ pilot symbols, with a distance of $\Delta = \lfloor \frac{K}{K_p - 1} \rfloor = 40$ subcarriers between pilot blocks. The channel comprised $L_{\mathrm{ch}} = 40$ i.i.d. standard normal taps (i.e., uniform delay power profile).

Fig. 12 shows the average BER versus the SNR E_b/N_0 for the proposed receiver, the conventional receiver, and the genie-aided receiver. In all cases, ten iterations were performed. It is seen that at SNRs larger than 10 dB, the proposed receiver performs virtually as well as the genie-aided receiver and about 5 dB better than the conventional receiver. For the proposed receiver and the conventional receiver, at an SNR of $E_b/N_0 = 13$ dB, Fig. 13 shows the mean square error (MSE) of the channel estimate and the BER versus the number of iterations. (For the proposed receiver, the channel estimate is given by $\overrightarrow{\mathbf{m}}(\mathbf{h}_{j,i}^{(u)})$.) It is seen that the channel estimation MSE of the proposed receiver decreases significantly after two iterations and saturates after about seven iterations, resulting in an MSE reduction of more than 6 dB compared to the conventional receiver. Correspondingly, after seven iterations,

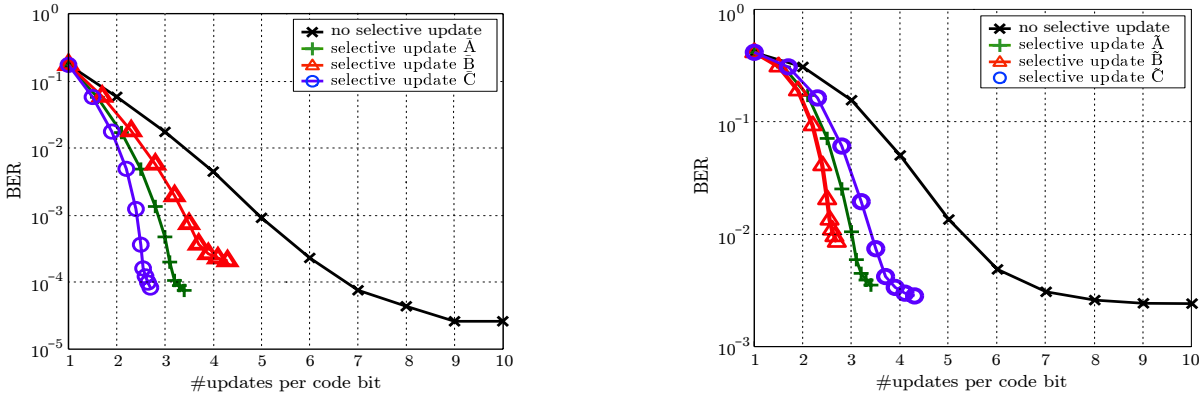

Fig. 11. BER versus average number of message updates for (a) user #1 and (b) user #2, obtained by receivers using different selective message update schemes and by the receiver without selective message updates ($M_{\mathrm{T}} = M_{\mathrm{R}} = 2$, $U = 2$, 16-QAM, $E_b/N_0 = 11$ dB). The receive SNR of user #1 is 3 dB higher than that of user #2.

the BER of the proposed receiver is about three orders of magnitude smaller than that of the conventional receiver.

Next, we show results for a SISO-OFDM-IDMA system with $U = 2$ users and 16-QAM modulation. The number of information bits was $J = 2048$, corresponding to $L = 8192$ code bits and $L_x = 2048$ 16-QAM symbols. The number of subcarriers was $K = 2156$, which left $K_p = 54$ pilot subcarriers for each user with a pilot distance of $\Delta = 40$ subcarriers. The channel had $L_{\mathrm{ch}} = 20$ i.i.d. standard normal taps. The receiver performed 15 iterations, and the messages $\overleftarrow{\mu}(\mathbf{H}^{(u)})$ were used for refining the channel estimate messages $\overrightarrow{\mu}(\mathbf{H}^{(u)})$ after the eighth iteration (empirically found to yield good performance). We consider three different fixed-complexity selective update schemes denoted $\bar{\mathrm{A}}$, $\bar{\mathrm{B}}$, and $\bar{\mathrm{C}}$. In these schemes, the number of message updates decreases in the course of the iterations, with scheme $\bar{\mathrm{A}}$ having the least aggressive decrease and scheme $\bar{\mathrm{C}}$ having the most aggressive decrease, i.e., $\alpha_{\bar{\mathrm{A}}} \geq \alpha_{\bar{\mathrm{B}}} \geq \alpha_{\bar{\mathrm{C}}}$ in each iteration. Fig. 14 shows the average BER versus the SNR E_b/N_0 for the proposed receiver (without selective updates and with selective updates according to scheme $\bar{\mathrm{B}}$), the conventional receiver, and the genie-aided receiver. It is seen that for a sufficiently high SNR, both versions of the proposed receiver outperform the conventional receiver by several dB, and they come close to the genie-aided receiver for E_b/N_0 higher than about 26 dB. Interestingly, the receiver with selective message updates performs better than the receiver with full message updates in spite of its significantly lower complexity (i.e., on average only 5.2 instead of 15 updates per code bit).

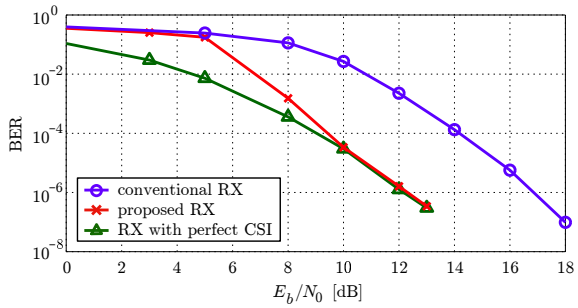

Fig. 12. BER versus SNR E_b/N_0 for different iterative receivers, for a SISO system with $U = 4$ users and BPSK modulation.

This behavior is further illustrated by Fig. 15, which shows the average BER versus the complexity (average number of message updates per code bit) for receivers employing the fixed-complexity selective update schemes $\bar{\mathrm{A}}$, $\bar{\mathrm{B}}$, and $\bar{\mathrm{C}}$ and for the receiver without selective updates, at an SNR of 25.5 dB. Surprisingly, schemes $\bar{\mathrm{A}}$ and $\bar{\mathrm{B}}$ exhibit a simultaneous performance improvement and complexity reduction: more specifically, after 15 iterations, their BER is one order of magnitude lower than that of the receiver without selective updates even though their complexity is smaller by roughly 50 % and 70 %, respectively. An increased BER is observed only if the complexity reduction is too strong: scheme $\bar{\mathrm{C}}$ terminates at about twice the BER and 20 % of the complexity of the receiver with full message updates. We conjecture that with fewer updates, the many cycles of the underlying factor graph have a smaller influence on the approximation accuracy of the sum-product algorithm, and that this effect explains the BER reduction achieved by schemes $\bar{\mathrm{A}}$ and $\bar{\mathrm{B}}$.

2) Multiple-antenna system: Finally, we consider a 2×2 MIMO-OFDM-IDMA system with $U = 4$ users and BPSK modulation. The number of information bits per user was $J = 512$ (corresponding to $L = 2L_x = 4096$ code bits or BPSK symbols). We used $K = 2800$ OFDM subcarriers of which 752 were pilot subcarriers (i.e., $K_p = 94$ pilots per user and transmit antenna), with a pilot block spacing of $\Delta = 30$ subcarriers. The matrix impulse response of the channel had $L_{\mathrm{ch}} = 30$ i.i.d. taps with i.i.d. standard normal elements. Fig. 16 compares the BER performance of the proposed receiver (without selective message update) with that of a conventional receiver (performing explicit channel estimation followed by iterative data detection) and that of a genie-aided receiver with perfect CSI. All three receivers performed ten iterations. It is seen that at SNRs above 12 dB, our receiver performs within 1 dB of the genie-aided receiver and gains about 5 dB over the conventional receiver.

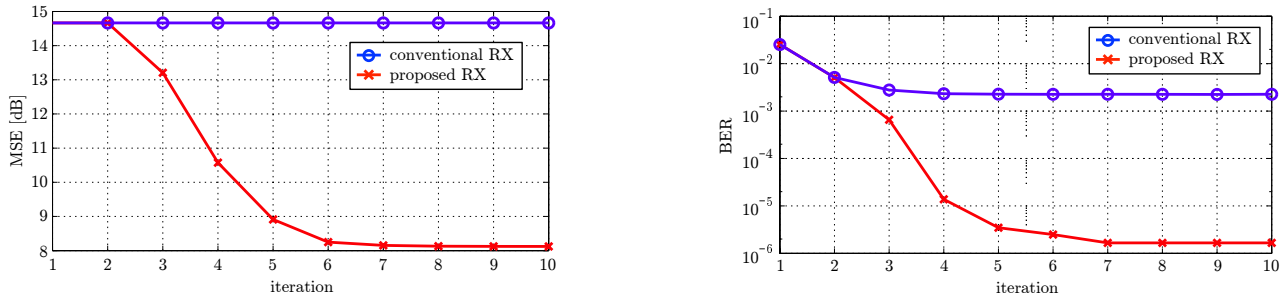

(a) (b)

Fig. 13. (a) Channel estimation MSE and (b) BER versus the number of iterations for the proposed receiver and the conventional receiver ($M_{\mathrm{T}} = M_{\mathrm{R}} = 1$, $U = 4$, BPSK, $E_b/N_0 = 13\,\mathrm{dB}$).

VII. Conclusion

Interleave-division multiple access (IDMA) recently became a promising alternative to code-division multiple access (CDMA) because of its potentially better performance and lower complexity. In this paper, we have used a factor graph/message passing framework and the sum-product algorithm to systematically devise an iterative receiver for IDMA in the context of multiple-input multiple-output orthogonal frequency division multiplexing (MIMO-OFDM) with higher-order modulation. The proposed receiver jointly performs pilot-aided channel estimation, multiuser detection, and channel decoding and provides a computationally feasible approximation of the MAP detector. The use of Gaussian message approximations results in a receiver complexity that scales only linearly with the number of users. A further significant complexity reduction is achieved by a novel selective message update scheme.

Simulation of the proposed MIMO-OFDM-IDMA receiver allowed us to estimate the maximum achievable rate and to compare it with the information-theoretic capacity of the multiple-access channel. It was seen that for low to medium signal-to-noise ratios, the achievable rate is close to the capacity. Furthermore, we presented simulation results assessing the bit error rate (BER) performance of the proposed receiver and the performance gains relative to a conventional iterative IDMA receiver performing separate channel estimation. Our simulations showed that the proposed turbo-like integration of channel estimation in the iterative soft multiuser detection and channel decoding scheme yields a dramatic improvement of reliability. Finally, we demonstrated that the proposed selective message update scheme offers a very favorable performance-complexity tradeoff, in the sense that low BERs can be obtained with a small average number of message updates per bit.

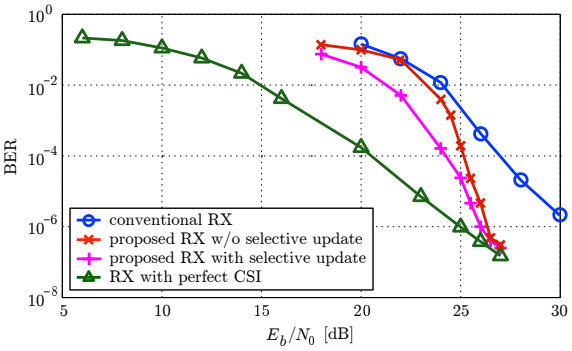

Fig. 14. BER versus SNR E_b/N_0 for different iterative receivers ($M_{\mathrm{T}} = M_{\mathrm{R}} = 1$, $U = 2$, 16-QAM).

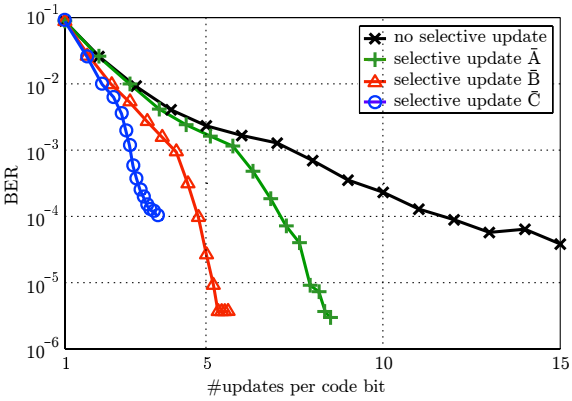

Fig. 15. BER versus average number of message updates for receivers with different selective message update schemes and without selective update ($M_{\mathrm{T}} = M_{\mathrm{R}} = 1$, $U = 2$, 16-QAM, $E_b/N_0 = 25.5\,\mathrm{dB}$).

References

[1] L. Ping, L. Liu, K. Wu, and W. K. Leung, "Interleave-division multiple-access," *IEEE Trans. Wireless Comm.*, vol. 5, pp. 938–947, April 2006.

[2] S. Verdú, *Multiuser Detection*. Cambridge (UK): Cambridge Univ. Press, 1998.

[3] L. Ping, "Interleave-division multiple access and chip-by-chip iterative multi-user detection," *IEEE Comm. Mag.*, vol. 43, pp. 19–23, June 2005.

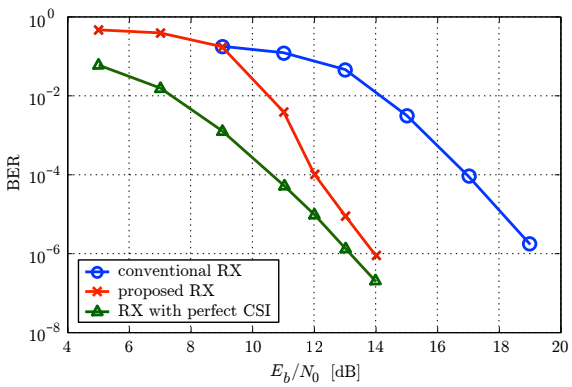

Fig. 16. BER versus SNR for different iterative receivers ($M_{\mathrm{T}} = M_{\mathrm{R}} = 2$, $U = 4$, BPSK).

[4] K. Kusume and G. Bauch, "CDMA and IDMA: Iterative multiuser detections for near-far asynchronous communications," in *Proc. IEEE PIMRC'05*, (Berlin, Germany), pp. 426–431, Sept. 2005.

[5] K. Kusume, G. Dietl, W. Utschick, and G. Bauch, "Performance of interleave division multiple access based on minimum mean square error detection," in *Proc. IEEE ICC-2007*, (Glasgow, UK), pp. 2961–2966, June 2007.

[6] B. Cristea, D. Roviras, and B. Escrig, "Turbo receivers for interleave-division multiple-access systems," *IEEE Trans. Comm.*, vol. 57, pp. 2090–2097, July 2009.

[7] K. Kusume, G. Bauch, and W. Utschick, "IDMA vs. CDMA: Detectors, performance and complexity," in *Proc. IEEE GLOBECOM'09*, (Honolulu, HI), Nov./Dec. 2009.

[8] C. Novak, F. Hlawatsch, and G. Matz, "MIMO-IDMA: Uplink multiuser MIMO communications using interleave-division multiple access and low-complexity iterative receivers," in *Proc. IEEE ICASSP-2007*, (Honolulu, HI), pp. 225–228, April 2007.

[9] I. Mahafeno, C. Langlais, and C. Jego, "OFDM-IDMA versus IDMA with ISI cancellation for quasi-static Rayleigh fading multipath channels," in *Proc. 4th Int. Symp. Turbo Codes and Related Topics*, (Munich, Germany), pp. 3–7, April 2006.

[10] L. Ping, Q. Guo, and J. Tong, "The OFDM-IDMA approach to wireless communication systems," *IEEE Wireless Comm.*, vol. 14, pp. 18–24, June 2007.

[11] C. Novak, G. Matz, and Hlawatsch, "Factor graph based design of an OFDM-IDMA receiver performing joint data detection, channel estimation, and channel length selection," in *Proc. IEEE ICASSP-2009*, (Taipei, Taiwan), pp. 2561–2564, April 2009.

[12] D. Hao and P. A. Hoeher, "Helical interleaver set design for interleave-division multiplexing and related techniques," *IEEE Comm. Letters*, vol. 12, pp. 843–845, Nov. 2008.

[13] K. Kusume and G. Bauch, "Simple construction of multiple interleavers: Cyclically shifting a single interleaver," *IEEE Trans. Comm.*, vol. 56, pp. 1394–1397, Sept. 2008.

[14] X. Zhou, Z. Shi, and M. C. Reed, "Iterative channel estimation for IDMA systems in time-varying channels," in *Proc. IEEE GLOBECOM'07*, (Washington D.C.), pp. 4020–4024, Nov. 2007.

[15] P. A. Hoeher, H. Schoeneich, and C. Fricke, "Multi-layer interleave-division multiple access: theory and practice," *European Trans. Telecomm.*, vol. 19, pp. 523–536, Aug. 2008.

[16] X. Wang and H. V. Poor, "Iterative (turbo) soft interference cancellation and decoding for coded CDMA," *IEEE Trans. Comm.*, vol. 47, pp. 1046–1061, July 1999.

[17] J. Boutros and G. Caire, "Iterative multiuser joint decoding: Unified framework and asymptotic analysis," *IEEE Trans. Inf. Theory*, vol. 48, pp. 1772–1793, July 2002.

[18] F. R. Kschischang, B. J. Frey, and H.-A. Loeliger, "Factor graphs and the sum-product algorithm," *IEEE Trans. Inf. Theory*, vol. 47, no. 2, pp. 498–519, 2001.

[19] H.-A. Loeliger, J. Dauwels, J. Hu, S. Korl, L. Ping, and F. R. Kschischang, "The factor graph approach to model-based signal processing," *Proc. IEEE*, vol. 95, pp. 1295–1322, June 2007.

[20] H. Wymeersch, *Iterative Receiver Design*. New York (NY): Cambridge University Press, 2007.

[21] A. P. Worthen and W. E. Stark, "Unified design of iterative receivers using factor graphs," *IEEE Trans. Inf. Theory*, vol. 47, pp. 843–849, Feb. 2001.

[22] M. C. Valenti and B. D. Woerner, "Iterative channel estimation and decoding of pilot symbol assisted turbo codes over flat-fading channels," *IEEE J. Sel. Areas Comm.*, vol. 19, pp. 1697–1705, Sept. 2001.

[23] N. Huaning, S. Manyuan, J. Ritcey, and L. Hui, "A factor graph approach to iterative channel estimation and LDPC decoding over fading channels," *IEEE Trans. Wireless Comm.*, vol. 4, pp. 1345–1350, July 2005.

[24] Y. Liu, L. Brunel, and J. J. Boutros, "Belief propagation with Gaussian approximation for joint channel estimation and decoding," in *Proc. IEEE PIMRC'08*, (Cannes, France), pp. 1–5, Sept. 2008.

[25] M. Zhao, Z. Shi, and M. C. Reed, "Iterative turbo channel estimation for OFDM system over rapid dispersive fading channel," *IEEE Trans. Wireless Comm.*, vol. 7, pp. 3174–3184, Aug. 2008.

[26] Y. Liu, L. Brunel, and J. J. Boutros, "EM channel estimation for coded OFDM transmissions over frequency-selective channel," in *Proc. IEEE ISSSTA'08*, (Bologna, Italy), pp. 544–549, Aug. 2008.

[27] Y. Liu, L. Brunel, and J. J. Boutros, "Joint channel estimation and decoding using Gaussian approximation in a factor graph over multipath channel," in *Proc. IEEE PIMRC'09*, (Tokyo, Japan), pp. 3164–3168, Sept. 2009.

[28] P. Schniter, "A message-passing receiver for BICM-OFDM over unknown clustered-sparse channels," *IEEE J. Selected Topics in Signal Processing*, vol. 5, pp. 1462–1474, Dec. 2011.

[29] G. E. Kirkelund, C. N. Manchón, L. P. Christensen, E. Riegler, and B. H. Fleury, "Variational message-passing for joint channel estimation and decoding in MIMO-OFDM," in *Proc. IEEE Globecom'10*, (Miami, FL), pp. 1–6, Dec. 2010.

[30] C. Knievel, P. A. Hoeher, A. Tyrrell, and G. Auer, "Multi-dimensional graph-based soft iterative receiver for MIMO-OFDM," *IEEE Trans. Comm.*, vol. 60, pp. 1599–1609, June 2012.

[31] G. Colavolpe, D. Fertonani, and A. Piemontese, "SISO detection over linear channels with linear complexity in the number of interferers," *IEEE J. Selected Topics in Signal Processing*, vol. 5, pp. 1475–1485, Dec. 2011.

[32] E. Zimmermann, G. Fettweis, P. Pattisapu, and P. K. Bora, "Reduced complexity LDPC decoding," in *Proc. Int. Symp. Wireless Personal Multimedia Commun. (WPMC'04)*, (Abano Terme, Italy), Sept. 2004.

[33] R. Bresnan, W. Marnane, and M. Sala, "Efficient low-density parity-check decoding," in *Proc. Irish Signals and Systems Conference*, (Belfast, Ireland), pp. 613–618, July 2004.

[34] A. Blad, O. Gustafsson, and L. Wanhammar, "An early decision decoding algorithm for LDPC codes using dynamic thresholds," in *Proc. European Conference on Circuit Theory and Design*, (Cork, Ireland), pp. 285–288, Aug. 2005.

[35] E. Cavus and B. Daneshrad, "A computationally efficient selective node updating scheme for decoding of LDPC codes," in *Proc. IEEE MILCOM'05*, (Atlantic City, NJ), pp. 1375–1379, Oct. 2005.

[36] E.-A. Choi, D.-I. Chang, D.-G. Oh, and J.-W. Jung, "Low computational complexity algorithms of LDPC decoder for DVB-S2 systems," in *Proc. IEEE VTC-2005*, (Dallas, TX), pp. 536–539, Sept. 2005.

[37] K. Shin and J. Lee, "Low complexity LDPC decoding techniques with adaptive selection of edges," in *Proc. IEEE VTC'07*, (Dublin, Ireland), pp. 2205–2209, April 2007.

[38] A. I. V. Casado, M. Griot, and R. D. Wesel, "LDPC decoders with informed dynamic scheduling," *IEEE Trans. Comm.*, vol. 58, pp. 3470–3479, Dec. 2010.

[39] C. Novak, G. Matz, and F. Hlawatsch, "A factor graph approach to joint iterative data detection and channel estimation in pilot-assisted IDMA transmissions," in *Proc. IEEE ICASSP-2008*, (Las Vegas, NV), pp. 2697–2700, April 2008.

[40] C. Novak, F. Hlawatsch, and G. Matz, "Low-complexity factor graph receivers for spectrally efficient MIMO-IDMA," in *Proc. IEEE ICC-2008*, (Beijing, China), pp. 770–774, May 2008.

[41] D. Tse and P. Viswanath, *Fundamentals of Wireless Communication*. Boston (MA): Cambridge University Press, 2005.

[42] J. G. Proakis, *Digital Communications*. New York (NY): McGraw-Hill, 3rd ed., 1995.

[43] L. R. Bahl, J. Cocke, F. Jelinek, and J. Raviv, "Optimal decoding of linear codes for minimizing symbol error rate," *IEEE Trans. Inf. Theory*, vol. 20, pp. 284–287, March 1974.

[44] T. M. Cover and J. A. Thomas, *Elements of Information Theory*. Hoboken (NJ): Wiley, 2nd ed., 2006.

[45] T. J. Richardson, M. A. Shokrollahi, and R. L. Urbanke, "Design of capacity-approaching irregular low-density parity check codes," *IEEE Trans. Inf. Theory*, vol. 47, no. 2, pp. 619–637, 2001.

Clemens Novak received the Dipl.-Ing. degree in electrical engineering and the Dr. techn. degree in communication engineering from Vienna University of Technology, Austria, in 2005 and 2010, respectively. From 2005 to 2010, he was a Research and Teaching Assistant with the Institute of Communications and Radio Frequency Engineering, Vienna University of Technology. Since 2010, he has been with Kapsch TrafficCom, Vienna, Austria. His research interests are in wireless communications with emphasis on MIMO multiuser systems, coded modulation, and iterative receivers.

Gerald Matz (S'95–M'01–SM'07) received the Dipl.-Ing. degree (1994) and the Dr. techn. degree (2000) in Electrical Engineering and the Habilitation degree (2004) for "Communication Systems" from Vienna University of Technology, Austria. He is currently an Associate Professor with the Institute of Telecommunications, Vienna University of Technology. He has held visiting positions with the Laboratoire des Signaux et Systèmes, Ecole Supérieure d'Electricité, France; with the Communication Theory Lab at ETH Zurich, Switzerland; and with Ecole Nationale Supérieure d'Electrotechnique, d'Electronique, d'Informatique et d'Hydraulique de Toulouse, France. He has published some 160 scientific articles in international journals, conference proceedings, and edited books. He is co-editor of the book *Wireless Communications over Rapidly Time-Varying Channels* (New York: Academic, 2011). His research interests include wireless communications, sensor networks, statistical signal processing, and information theory.

Prof. Matz currently serves on the *IEEE SPS Technical Committee on Signal Processing for Communications and Networking* and on the *IEEE SPS Technical Committee on Signal Processing Theory and Methods*. He is Associate Editor of the IEEE TRANSACTIONS ON INFORMATION THEORY and was on the Editorial Board of the IEEE TRANSACTIONS ON SIGNAL PROCESSING, the EURASIP Journal SIGNAL PROCESSING, and the IEEE SIGNAL PROCESSING LETTERS. He was Lead Guest Editor of the *Special Issue on Managing Complexity in Multiuser MIMO Systems* in the IEEE JOURNAL OF SELECTED TOPICS IN SIGNAL PROCESSING, Technical Program Co-Chair of EUSIPCO 2004, Technical Vice-Chair of Asilomar 2013, and member of the Technical Program Committee of numerous international conferences. In 2006, he received the Kardinal Innitzer Most Promising Young Investigator Award. He is a Senior Member of the IEEE.

Franz Hlawatsch (S'85–M'88–SM'00–F'12) received the Diplom-Ingenieur, Dr. techn., and Univ.-Dozent (habilitation) degrees in electrical engineering/signal processing from Vienna University of Technology, Vienna, Austria in 1983, 1988, and 1996, respectively. Since 1983, he has been with the Institute of Telecommunications, Vienna University of Technology. During 1991–1992, as a recipient of an Erwin Schrödinger Fellowship, he was a visiting researcher with the Department of Electrical Engineering, University of Rhode Island, Kingston, RI, USA. In 1999, 2000, and 2001, he held one-month visiting professor positions with INP/ENSEEIHT, Toulouse, France and IRCCyN, Nantes, France. He (co)authored a book, two review papers that appeared in the IEEE SIGNAL PROCESSING MAGAZINE, about 200 refereed scientific papers and book chapters, and three patents. He coedited three books, including *Time-Frequency Analysis: Concepts and Methods* (London: ISTE/Wiley, 2008) and *Wireless Communications over Rapidly Time-Varying Channels* (New York: Academic, 2011). His research interests include signal processing for wireless communications and sensor networks, statistical signal processing, and compressive signal processing.

Prof. Hlawatsch was Technical Program Co-Chair of EUSIPCO 2004 and served on the technical committees of numerous IEEE conferences. He was an Associate Editor for the IEEE TRANSACTIONS ON SIGNAL PROCESSING from 2003 to 2007 and for the IEEE TRANSACTIONS ON INFORMATION THEORY from 2008 to 2011. From 2004 to 2009, he was a member of the IEEE SPS Technical Committee on Signal Processing for Communications and Networking. He is coauthor of papers that won an IEEE Signal Processing Society Young Author Best Paper Award and a Best Student Paper Award at IEEE ICASSP 2011.